Title

Near-census ecohydraulics bioverification of *Oncorhynchus mykiss* spawning microhabitat preferences

Journal

Journal of Ecohydraulics, 1

ISSN

2470-5357

Authors

Kammel, Leah E
Pasternack, Gregory B
Massa, Duane A
et al.

Publication Date

2016-09-13

DOI

10.1080/24705357.2016.1237264

Data Availability

The data associated with this publication are available upon request.

Peer reviewed

Near-census ecohydraulic bioverification of *Oncorhynchus mykiss* spawning microhabitat preferences.

Authors: Leah E. Kammel[1], Gregory B. Pasternack[1]*, Duane A. Massa[3], Paul M. Bratovich[2]

Affiliations:

[1]Department of Land, Air, and Water Resources, University of California at Davis, Davis, CA 95616, USA

[2]HDR, Inc., 2031 Howe Ave, Suite 110, Sacramento, CA 95825, USA

[3]Pacific States Marine Fisheries Commission, 2711 Highway 20, Marysville, CA 95901, USA

*Corresponding author

Citation: Kammel, L., Pasternack, G. B., Massa, D., Bratovich, P. 2016. Near-census ecohydraulic bioverification of Oncorhynchus mykiss spawning microhabitat preferences and avoidances. Journal of Ecohydraulics, doi: 10.1080/24705357.2016.1237264.

Abstract

There is increasing scientific and management interest in Oncorhynchus mykiss habitat use, as this species has become rare and elusive due to anthropogenic impacts on regional populations. Past research defined general physical habitat conditions utilized by spawning O. mykiss, but modern science and management require spatially explicit predictive capability. Meanwhile, ecohydraulic prediction in general lacks objective, transparent bioverification, defined as assessment of the complete performance of a physical habitat model relative to observed biological utilization. This study developed a robust framework for ecohydraulic bioverification and applied it to improve the understanding of O. mykiss spawning. The testbed was 35.2 km of the regulated gravel-cobble lower Yuba River, California. Using two-dimensional hydrodynamic modelling, substrate mapping, and a two-year survey of O. mykiss redds, microhabitat representations were tested for their ability to predict spawner preference and avoidance. O. mykiss redds showed a strong preference for mean water column velocities of 0.36-0.69 m/s and depths of 0.38-0.84 m. The substrate range preferred for O. mykiss spawning was within 32-90 mm. O. mykiss spawning microhabitat predictions passed multiple bioverification tests enabling development of a habitat area versus discharge relation that showed that the lower Yuba River has ample O. mykiss spawning habitat.

Keywords: ecohydraulics, 2D habitat modelling, salmon spawning, aquatic habitat, river modelling

1 Introduction

Oncorhynchus mykiss (*O. mykiss*) is a salmonid species native to tributaries along North American and Asian Pacific coasts. Prior to dam construction, water development and anthropogenic watershed perturbations, the anadromous form of *O. mykiss* (i.e. steelhead) was distributed throughout the Sacramento and San Joaquin rivers in the Central Valley of California, bounded by the Sierra Nevada to the east and the Coast Ranges to the west (Busby et al. 1996; McEwan 2001). The California Central Valley steelhead Distinct Population Segment was listed as threatened under the U.S. Endangered Species Act in 1998 (Good et al. 2005).

The National Marine Fisheries Service (NMFS) (2009) reported that over the last 30 years, steelhead populations in the upper Sacramento River have substantially declined. Many factors have contributed to their decline. McEwan (2001) and Lindley et al. (2006) concluded that the single greatest stressor was the loss of spawning habitat due to impassable dams, which blocked access to an estimated 80% of the historical *O. mykiss* spawning habitat in the Central Valley of California. Protection and enhancement of the spawning habitat that remains hinges on understanding the physical conditions preferred for spawning locations, and ensuring that these conditions are abundant in river reaches accessible to *O. mykiss*. However, now that these fish are rare and elusive, obtaining data on their wild behaviours and habitat needs is challenging compared to abundant salmonid species. A traditional statistical sampling campaign or local site study would not observe enough individuals to yield statistically robust conclusions. To solve the problems associated with their rarity, this study developed new methods for evaluating the predictive ability of evidence-driven ecohydraulic models of spawning habitat quality, and applied these methods to evaluate how well *O. mykiss* spawning behaviour is understood. These

methods work for abundant species as well, but may not be needed if simpler sampling strategies are robust for them.

1.1 Microhabitat concepts

Microhabitat features are point-scale measurements of physical habitat attributes that are utilized by organisms while performing an ecological function. Local hydraulics (Burner 1951; Beland et al. 1982; Crowder & Diplas 2006), riverbed substrate (Kondolf & Wolman 1993), and in-gravel physical chemistry (Merz and Setka 2004) have been found to be important physical factors (i.e. "physical habitat") affecting *O. mykiss* spawning site selection at the microhabitat scale. Local water depth, velocity, and riverbed substrate size may have the most direct and largest impact on point-scale spawning site selection. This might be pre-conditioned by landform and flow features at the channel width scale (i.e. "mesohabitat") (Geist & Dauble 1998; Hanrahan 2007; Moir & Pasternack 2008) and larger River Styles scale (Thomson et al. 2004), but even within a mesohabitat patch a spawner's exact site selection is likely not random (Elkins et al. 2007). Though not specific to *O. mykiss*, there is evidence that spawning site selection by salmonids is behaviourally influenced to produce clustering within preferred habitat (Essington et al. 1998; Mull & Wilzbach 2007).

Many studies have shown that salmonids select spawning locations largely based on external physical attributes of the aquatic environment at various spatial scales. A general range of suitable water velocities for *O. mykiss* spawning as analyzed by previous studies is 0.30 to 1.34 m/s (Briggs 1953; Smith 1973; Swift 1976; Bovee 1978; USFWS 1996, 1997, 2007). Suitable water depths are reported to range from 0.10 to 1.0 m (Briggs 1953; Sams & Pearson 1963; Smith 1973; Swift 1976; USFWS 1996, 1997, 2007). Suitable substrate sizes compiled from several past studies of *O. mykiss* spawning range from 10.4 to 152.4 mm, which spans gravel and

cobble size ranges (Burner 1951; Briggs 1953; Chambers et al. 1954; Chambers et al. 1955; Orcutt et al. 1968; Cederholm & Salo 1979; Shirazi & Seim 1981; Kondolf & Wolman 1993). How well these ranges apply in a predictive modelling framework is unknown.

1.2 Near-census river science

The ability to collect topographic data and map large areas quickly and inexpensively at the meter scale is growing rapidly. It is just a question of time until meter-scale topography for the whole world is available, and the use of high-resolution topographic mapping in many scientific fields is an exciting frontier of current research. The term 'near-census' is used herein to refer to comprehensive, spatially explicit, process-based approaches using the 1-m scale as the basic building block for investigating rivers in light of the emerging abundance of meter-scale topographic datasets. The concept of a 'near-census' implies that meter-scale data represent variables in a level of detail that approaches the population of conditions, but that there remains a finer level of detail in the domain of continuum mechanics that eventually will be resolved with further technological developments that will constitute full 'census' data collection.

Near-census mapping and numerical modelling require that topographic data collection is done fully and mindfully, so that terrain complexity at the 1-m scale is represented in subsequent 2D or 3D hydrodynamic and/or morphodynamic simulations and analyses. Near-census river science aims to represent key parameters of multiple spatial scales of a river at a high enough resolution so that uncertain interpolations and extrapolations are minimized (Gonzalez et al. 2015).

1.3 Study objectives

This study was conducted to apply established and emerging ecohydraulic methods to characterize and quantify the physical habitat conditions that influence spawning site selection,

and are preferred or avoided by spawning *O. mykiss* at the microhabitat scale. The influences of physical conditions and processes on spawning habitat selection were assessed by developing a predictive two-dimensional (2D) planimetric physical habitat model based on 2D hydraulics and microhabitat suitability for 35.2 km of river at ~ 1-m resolution, which is considered a near-census of habitat for adult *O. mykiss* spawners. A new bioverification procedure was developed and used to determine beyond the 95% statistical confidence level if *O. mykiss* spawners actually used the areas indicated by the model to be preferred habitat, and did not use the areas indicated to be nonhabitat or low-quality habitat. The bioverified model that accurately predicted *O. mykiss* spawning habitat utilization was used to quantify how spawning habitat area varies with discharge on a near-census basis, in contrast to indices developed from limited sampling, which differentiates this procedure from the traditional use of the weighted usable area (WUA) metric. Although 2D microhabitat studies are not new, past efforts lacked a robust framework for bioverification and thus were likely not statistically justified for use in assessing small populations with a quantified level of uncertainty. This study developed new bioverification ideas and a bioverification framework for wider use as a novel contribution in addition to improving the understanding of *O. mykiss* spawning habitat. Also, the size of river segment (35.2 km) and study resolution (1 m) tested the feasibility of scaling up ecohydraulic analysis from short sites to long river segments. There is great value in the application of near-census physical habitat modelling at this scale and resolution in studying rare populations, as the near-census approach removes the problem of under-sampling or missing observations of rare populations that is inherent to traditional small-scale site or reach surveys.

2 Study Site

The Yuba River drains 3480 km^2 of the western slope of the Sierra Nevada, including portions of Sierra, Placer, Yuba, and Nevada counties. There is a long history of human disturbance in the watershed, including hydraulic gold mining that transformed the lower Yuba River with the deposition of millions of tons of mining sediment during the mid to late nineteenth century (Gilbert 1917; Curtis et al. 2005; James et al. 2009). The lower Yuba River is the 37.1 km river segment extending downstream from Englebright Dam to its confluence with the Feather River near Marysville, California (Fig. 1). Englebright Dam, an 85-m concrete arch dam built in 1941, is an impassable barrier for fish and marks the upstream extent of habitat available to *O. mykiss*. The lower Yuba River is a regulated, wandering gravel/cobble bed river that is meandering to straight in pattern, with a high width-to-depth ratio and slight to no entrenchment (Wyrick & Pasternack 2012). The segment's overall bed slope and mean bed material grain size are 0.185% and 97 mm, respectively.

The Yuba River catchment is thought to have historically supported a large *O. mykiss* population prior to aggressive anthropogenic impacts that began with the 1848 Californian Gold Rush. Today, a residual interbreeding population of both anadromous steelhead and resident rainbow trout, collectively referred to as *O. mykiss*, are present in the lower Yuba River and the progeny of both may exhibit either life history (Zimmerman et al. 2009; Mitchell 2010; YARMT 2013). *O. mykiss* in the lower Yuba River may be exhibiting a predominately residential life history pattern due to the managed low water temperatures and favourable selection strategy relative to anadromy (YARMT 2013). The elasticity of *O. mykiss* life history strategies within a single population differ from other salmonids, which are primarily anadromous. Although the *O. mykiss* in the lower Yuba River have been widely stated to be one of the largest remaining wild

populations in the Central Valley (Kozlowski 2004), YARMT (2013) found that a substantial amount of straying hatchery-origin steelhead also utilize the lower Yuba River and concluded that the current *O. mykiss* population likely does not represent a pure ancestral genome.

3 Methods

The study's overall experimental design is portrayed in Figure 2. Because this study was funded by and used for local management, it was built in United States customary units, so reported SI values may seem unusual. A key challenge for interdisciplinary ecohydraulic research is that it requires many diverse field and modelling methods to be integrated, yet journal articles are by necessity brief. This article balances the need for transparency with limited space by presenting essential concepts and leaving full details to the Supplementary Materials and a technical report (Kammel & Pasternack 2014) publicly available at http://www.yubaaccordrmt.com/default.htm.

3.1 *O. mykiss* spawning observations

In this study, the selection of physical conditions by spawning *O. mykiss* was indicated by the presence and location of an individual redd, which is composed of the riverbed depression into which eggs are laid, and the associated tailspill. Redd surveys are a standard tool for investigating salmonid populations and physical habitat throughout the Pacific region of the United States (e.g. Boydstun & McDonald 2005; Gallagher et al. 2007). Census redd surveys were conducted weekly during the *O. mykiss* winter spawning season of 2010 by boat and snorkeling according to a protocol (Campos & Massa 2009) available at the above website. Additional surveys were conducted during 2011, but were inconsistent due to high flows and turbid conditions. A total of 261 redds were observed, with 223 sightings from January through April of 2010 and 38 sightings during the same months in 2011. These low numbers are

171 indicative of a rare, elusive population and are roughly one-tenth of those for fall-run Chinook
172 salmon observed in the preceding autumnal Chinook spawning season. The geographic location
173 of each observed redd was recorded with a meter-scale Trimble GeoXH or GeoXT differential
174 GPS. Annual *O. mykiss* redd survey findings are reported in Campos and Massa (2011, 2012).

175 Lower Yuba River hydrology varied significantly during the study, with discharges from 19.8 to
176 130.2 m^3/s and 57.3 to 643.0 m^3/s observed from January to April of 2010 and 2011, respectively
177 (see Supplementary Materials section 1.1). *O. mykiss* spawn during the winter rainy season,
178 when discharges can be highly variable and therefore the range of hydraulic conditions
179 experienced by spawners at a specific location in the lower Yuba River would not be well
180 represented using the average discharge over the period. Due to this variability in discharge,
181 spawning observations were grouped with others around a similar discharge so conditions
182 experienced during redd building could be analyzed using a single 2D habitat model with a
183 representative discharge. There were three groups of observed redds that could be analyzed with
184 a single representative modeled discharge for each group (Table 1). Each of the three redd
185 groups provides a small but sufficient sample size by which to test the physical habitat model
186 predictions at three distinct discharges. The representativeness of each flow was carefully
187 investigated and the effect on water depth and velocity of using a slightly different discharge
188 than that observed for any given day was only 0.35% to 1.9%, which was too low to affect study
189 results. By comparison the mean unsigned errors in depth and velocity reported in the validation
190 analysis below are an order of magnitude higher, and typically 10% to 30% in the literature as a
191 whole. Also, depth and velocity data are binned into broad ranges for habitat analysis, which also
192 significantly reduces the effect of small uncertainties in their values.

3.2 Abiotic data

Abiotic data were used to characterize the attributes of locations in the river and validate the 2D hydrodynamic model. For each dataset described below, extensive critical thinking, methodological testing, and quality assurance and quality control procedures were undertaken, as detailed in public technical reports at the above website. Abiotic data in this study included topography/bathymetry, substrate size, and hydraulics. A brief summary is provided, with details in Supplementary Materials section 1.2.

The most important element was a previously published ~1-m resolution digital elevation model (DEM) of the entire lower Yuba River corridor, including the submerged topography of the channel bed (Carley et al. 2012; Abu-Aly et al. 2013; Wyrick & Pasternack 2014, 2015). The DEM excludes a short hazardous section of rapids in the Narrows Canyon. Ground-based, boat-based, and remote sensing data collection protocols used professional best practices (Pasternack 2009; see Supplementary Materials section 1.2).

Substrate data consisted of a system-wide facies map, with each field-mapped polygon having a visual grain size characterization based on a carefully tested protocol (Jackson et al. 2013). Grain size data consisted of the percent abundance (to within the nearest 10 %) of six different size classes easily differentiated by a thoroughly trained and tested field crew (0-0.0625, 0.0625-2, 2-32, 32-90, 90-128, 128-256, and >256 mm). Crew performance in multiple tests against measured samples was quantified and excellent. These size classes were suitable for computing a mean grain size (D_{mean}) for each patch and conversion to a raster with the same resolution as the DEM (Jackson et al. 2013; Pasternack et al. 2014).

Hydraulic data (i.e. water surface elevations, depths, and velocity vectors) were collected using traditional and novel methods for evaluating the performance of the 2D hydrodynamic model. Airborne LiDAR and RTK GPS were used to obtain water surface elevations, while traditional cross-sectional surveys were used to obtain depths and depth-average velocity at 199 locations. In addition, a more novel method using Lagrangian particle tracking and RTK GPS mounted on a floating kayak was used to collect 5780 measurements of the surface velocity vector. Data were collected spanning an order of magnitude of discharge from the typical base flow to above bankfull flow (~14 to 170 m^3/s), which covered the range modeled in this study, except for the lowest flows evaluated for habitat, which were too low to be observed under the managed flow regime in the years of the study.

3.3 2D hydrodynamic model

The Surface-water Modelling System (SMS v. 10.1; Aquaveo, LLC, Provo, Utah, USA) and Sedimentation and River Hydraulics-two-dimensional (SRH-2D v. 2.1; Lai 2008) models were used to produce steady state 2D hydrodynamic models spanning the whole regulated lower Yuba River (except for the short unmapped rapids in the Narrows Canyon) according to best-practice procedures of Pasternack (2011) (see Supplementary Materials section 1.3 for model details). Different subsets of the 2D model results were used in recent journal articles by Abu-Aly et al. (2013), Gonzalez and Pasternack (2015), and Wyrick & Pasternack (2014, 2015). For this study, model outputs at each point at each discharge were used to create 0.914-m resolution raster maps with values of water depth and mean column velocity using the methods of Pasternack (2011), which involve steps related to isolating just the points in the wetted area from those that are dry and interpolating from an irregular point cloud to a raster grid. Table 1 indicates the steady discharges modeled for each observed *O. mykiss* spawner group. Model runs were also done for

21 flows ranging from 8.5 to 141.58 m^3/s to establish the relation between habitat abundance and discharge within the bankfull channel. The specific flows chosen included those for which validation data existed as well as those chosen by a committee of experts who serve as the river managers. There are more intervals at lower flows where there was expected to be more variation in habitat abundance and distribution and fewer at higher flows expected to have less variation.

Extensive hydraulic model validation was performed for unvegetated model simulations for an order of magnitude of flow range from base to over bankfull flow at locations away from vegetation using procedures explained in Pasternack (2011). Tests were done on mass conservation, water surface elevation (WSE), depth, velocity magnitude, and velocity direction (Barker 2011), with results tabulated in Supplementary Materials section 1.3. From cross-sectional surveys, predicted versus observed depths yielded a moderately strong coefficient of determination (r^2) of 0.66, and a reasonable median unsigned error of 17%. From the far more extensive Lagrangrian particle tracking dataset, predicted versus observed depth-averaged velocity magnitude yielded a strong r^2 value of 0.79 and a reasonable median unsigned error of 16%. Velocity direction tests yielded a strong r^2 value of 0.80 and an excellent median unsigned error of 4%. Overall, the lower Yuba River 2D models met or exceeded professional performance standards, but of course models have inherent limitations, with the worst problem being elevation data gaps (Anderson & Bates 1994; Pasternack et al. 2006).

3.4 Habitat Suitability Prediction

Habitat suitability assessment links measurable physical conditions at discrete locations with the ecological functionality of those locations. A habitat suitability curve (HSC) is a mathematical function governing such a linkage, with values ranging from 0 (non-habitat) to 1 (highly suitable habitat) across the range of possible values for the relevant physical habitat variable (or set of

variables). HSCs are extensively used in habitat studies and instream flow assessments (Bovee 1996; Bovee et al. 1998). HSCs can be developed to characterize how a population is actually distributed in an existing area (reflecting the tendency for an organism to prefer or avoid specific local conditions) or to idealize the functionality of nonexistent conditions. Furthermore, they can be evidence-based (e.g. Leclerc et al. 1995), expert-based (e.g. Baldridge 1981; Noack et al. 2013), or a combination of the two. Evidence-based HSCs are usually combinations of univariate functions, but for large datasets and/or diverse fish aquatic assemblages they can also be multivariate (Parasiewicz & Walker 2007).

For *O. mykiss* spawning, one of the most cited of HSCs is from Bovee (1978), which developed curves for depth, velocity, temperature, and substrate size from data compiled from various sources. Those HSCs have been utilized widely, because they are provided with the physical habitat simulation (PHABSIM) modelling package. However, the use of these standard curves has been found to introduce significant bias to instream flow results for streams of different sizes, and may not adequately represent microhabitat selection in all streams (e.g. Annear & Conder 1984; Vondracek & Longanecker 1993). As a result, local evidence-based, univariate hydraulic HSCs were developed using a non-parametric tolerance limits approach applied to depth (n=242) and velocity (n=236) at locations that motile *O. mykiss* adult spawners chose for reproduction on the lower Yuba River during 2010 and 2011 (Fig. 3a, b). The number of observations used for HSC development does not match the total number of observed redds (n=261) due to field conditions that prevented measurement of depth and velocity during some redd surveys and removal of some erroneous values caused by flow meter malfunction. Also, given the small population present, it was necessary to use all available data to produce HSCs instead of withholding a substantial amount for isolated use in bioverification, because the effect

283 of small data size would be too harmful in both required steps at that point. This is a reality in
284 working with rare, elusive populations.

285 Kondolf and Wolman (1993) found that *O. mykiss* prefer to spawn in small gravel to cobble-
286 sized substrate, with a median diameter ranging from 10.4 to 46.0 mm. They also suggested that
287 salmonids can spawn in substrates with a median diameter up to 10 % of fish length. Given that
288 observations of fork length of *O. mykiss* using a Vaki Riverwatcher system on the lower Yuba
289 River yield a range of fish sizes from 180-600 mm, this 10 % benchmark produces estimates of
290 the suitable bed material size of ~18-60 mm (Massa et al. 2012). Eight different substrate-size
291 HSCs were developed with the substrate dataset (using a combination of evidence and expert
292 judgment). Although they were all evaluated as part of the methodological developments in this
293 study, it is necessary for brevity to only report and use the most successful one herein. This best
294 performer was assigned a suitability value of 1 for the range of D_{mean} from 32-90 mm and an
295 intermediate suitability of 0.4 for the D_{mean} range of 90-200 mm. Although it may seem
296 surprising that this coarser material would be used, Moir & Pasternack (2010) reported that
297 Chinook salmon on the lower Yuba River exhibit an elastic multivariate preference in which
298 spawners will prefer coarser substrate when velocities are higher, so it is likely the same
299 behaviour is exhibited by *O. mykiss*. All values of D_{mean} outside of these ranges have a suitability
300 of 0. For full results for the other substrate HSCs evaluated, see Kammel & Pasternack (2014).

301 Hydraulic HSCs were turned into piecewise equations and applied to 2D depth and velocity
302 rasters, yielding univariate habitat suitability index (HSI) rasters. The substrate HSC for D_{mean}
303 was applied to the D_{mean} substrate raster in the same manner to create a raster of substrate HSI.
304 The geometric mean of the three hydraulic and substrate HSI rasters was computed to yield a

combined habitat suitability index (CHSI) raster. Rasters of CHSI are the final spatially explicit predictions of spawning habitat quality.

Recognizing that 2D hydrodynamic models are more precise than accurate, and that HSCs also contain uncertainties, it helps to lump HSI values into ranges to avoid the false impression that precise HSI values predict meaningful differences in organism behaviour (e.g. HSI values of 0.45 and 0.46 are not ecologically different). Past studies have recommended different schemes for lumping HSI values (Leclerc et al. 1995; Pasternack 2011). A new method is proposed in this study by which the created HSI bins are part of the model subject to evaluation and either affirmation or rejection. Each bin is usually interpreted in terms of a habitat quality. In this study, six habitat quality classes were delineated by binning HSI values in even intervals of 0.2, also considering a value of 0 as its own bin (Table 2). This scheme was tested per the procedures in the next section.

4 Bioverification Tests

A key novel aspect of this study is the formal introduction of specific "bioverification" tests and performance criteria, including development of statistical confidence limits that are more rigorous than past studies have reported. The term bioverification is introduced in place of the more commonly used term validation, because there are multiple components of a physical habitat model and it is helpful to have a different term for each major element. The term validation, which is heavily used in engineering and hydrology, is reserved in this study specifically for the requisite assessment of hydrodynamic model performance. The term bioverification is used for evaluating the complete performance of the physical habitat model relative to observed biological utilization. If the same term is used for both analyses, then no one

will know what was actually tested, whereas this way it is clear that validation relates to hydraulics and bioverification relates to overall habitat quality prediction performance, including hydraulics, HSCs, HSIs, and HSI binning.

The statistical methods that are used in this study are not new to science, but how they are adapted and formalized for use in ecohydraulics is new and imperative for advancement of the discipline. It is essential for ecohydraulics that more scientific effort be placed on developing and applying bioverification tests to increase confidence in the predictions that will be the foundation for important interdecadal to centennial decision-making regarding instream flow requirements. Two common tests of bioverification, the Mann-Whitney U test and an electivity index test, served as starting points for further developments in this study to test the 2D physical habitat model for *O. mykiss* spawning. Both tests are common when bioverification is attempted, so the main novelty herein relates to a significant expansion and scientific improvement of the electivity index test compared with how it has been used in the past.

4.1 Mann-Whitney U Test

The Mann-Whitney U test is a non-parametric statistical test to compare the distributions of two independent samples using rank sums, specifically by testing whether one distribution is stochastically greater than the other (Mann & Whitney 1947). This is a common, simple test to run that is also the easiest test for a physical habitat model to pass – if a model fails this test it should be thoroughly evaluated for the sources of failure and then re-made and tested again. The test was used to evaluate the statistical significance of the differentiation in habitat quality between utilized and non-utilized locations in the physical habitat model. The locations of redds in the three groups, Q_{low}, Q_{mid}, and Q_{high} make up three datasets of utilized locations, with n=43, 54, and 94, respectively. The ETGeowizards add-on (ET Spatial Techniques, Pretoria, South

Africa) to ArcGIS (v.10.1) was used to create a set of randomly distributed points (without replacement) of the same sample size as each of the three redd groups. The points in these datasets were randomly distributed anywhere within the wetted area of the corresponding discharge (even at observed spawning locations with equal probability as anywhere else), and served as a random selection of non-utilized locations, because they did not in fact include any of the actual observed spawning locations (as expected given the vast size of the point population). HSI values at the utilized and non-utilized locations for the three discharges were extracted from each physical habitat model, and the HSI values were ranked from smallest to largest. The Mann-Whitney U test was performed with a significance level of 5 % (two-sided). Tests with a p-value < 0.05 were considered to exhibit a statistically significant difference between the median HSI for utilized and non-utilized locations for the given physical habitat model, and thus passed bioverification.

Because this test only determines that there is a statistically significant difference between the utilized or non-utilized locations, it is necessary to take an additional step and assess which of those has the larger HSI value. Physical habitat models with a statistically significant Mann-Whitney U test result were thus used to calculate the median HSI values of the utilized and non-utilized locations. Physical habitat models that had higher median HSI for utilized locations than non-utilized ones were considered further bioverified.

4.2 Electivity and the forage ratio test

4.2.1 Forage ratio concept

The most restrictive test of bioverification used herein was a test of electivity using the forage ratio (FR), but with new developments compared to past studies. The FR was originally defined

372 to indicate an organism's preference or avoidance for a certain type of prey (Savage 1931;
373 Shorygin 1939; Hess & Swartz 1940; Ivlev 1961), but has been adapted and widely used as a
374 metric of electivity in ecology to determine resource and habitat selection behaviour (e.g.
375 Williams and Marshall 1938; Johnson 1980; Kobayashi et al. 2008). For use in ecohydraulics,
376 the FR is defined as the ratio of percent utilization ($\%U_i$) to percent available area ($\%A_i$), where
377 "i" indicates a specific habitat quality class according to the 0.2 interval CHSI bins. Percent
378 utilization is calculated as the number of redds observed within each habitat quality class divided
379 by the total number of redds. Percent available area is calculated as the wetted area that is
380 predicted to be within each habitat quality class divided by the total wetted area at the discharge
381 of interest.

382 The FR is easily interpreted. An FR equal to 1 represents a uniform distribution of redds, with
383 the percent occurrence exactly proportional to the percent available area in that domain. Given a
384 random chance of the occurrence of redds in a habitat quality class (FR=1), there is no
385 preference or avoidance of the area with that habitat quality. An FR value >1 indicates
386 preference for the habitat quality class, as it is being utilized in a greater proportion than it is
387 available in the landscape, while an FR value <1 indicates avoidance, as it is being utilized in a
388 smaller proportion than it is available in the landscape.

389 For values that are higher or lower than 1, FR values indicate the percent deviation from random
390 chance. For example, an FR of 1.5 indicates that the percent occurrence is 50% greater than
391 would be expected from random occurrence and a value of 0.5 indicates that the percent
392 occurrence is 50 % less than what would be expected.

A criticism of this FR test is the dependence on percent available area in each domain, which can be difficult to accurately quantify in studies that rely on transect sampling and interpolation to estimate the habitat available in reaches. This issue is greatly diminished by using near-census modelling. The FR is also criticized for theoretically ranging from 0 to infinity, with very high FR values resulting not from a high preference, but from extremely low availability. This can be avoided by adding a constraint wherein habitat quality classes that have <1% of the total available area are excluded from FR analysis, which effectively limits the FR to a maximum value of 100. In this study the highest FR value was <4, so this limit was not close to being utilized. Overall, the FR metric provides a simple, easy-to-understand metric of preference and avoidance and was highly suitable for this study, but in each case, a suitable electivity index should be carefully selected.

4.2.2 Bootstrapping test

Most studies that use the FR as a measure of electivity index define preference as having FR > 1, and avoidance as having FR < 1 (Lechowicz 1982; Deudero & Morales-Nin 2001; Estep et al. 2011). However, the odds of FR values exactly equaling 1 under random organism behaviour are very low, especially for a small population, and hence it is essential to evaluate how far an FR value must be from one before a habitat quality class may be identified as preferred or avoided. For small datasets, statistical reasoning dictates that the FR value must be further from 1 in order to indicate statistically significant preference or avoidance, because the fewer data points are used, the greater the possibility of a random occurrence of FR deviating strongly from 1. Thus, a statistical tool is needed to determine the thresholds of deviation from FR=1 that must be exceeded for an ecological interpretation to be made.

Statistical bootstrapping is a method for assigning a measure of accuracy to sample estimates (Efron & Tibshirani 1993) that has rarely been applied to determine confidence intervals on ecological indices (e.g. Dixon 1998). When data of a given size are used to calculate any test metric, such as physical habitat models and redd locations used to calculate the FR, bootstrapping can be used to quantify the statistical confidence limits to show that the data are non-random. To do this, many random sets of the same sample size as the real dataset are created and used to compute the test metric. With enough random sets, the statistical distribution of the test metric values for the random datasets should be a normal distribution, and a mean and standard deviation can be calculated.

Considering the small sample sizes in this study, ranging from n=43 (for an individual redd group) to n=261 (for the total number of observations), statistical bootstrapping was done for 10 random sets and the results were used to yield 95 % confidence threshold values of FR for each habitat quality class that indicate statistically significant results for the FR values of the observed data. The upper confidence limit, taken as the preference threshold, was computed as $\mu+2\sigma$, where μ is the mean FR value in the habitat quality class from the 10 random sets and σ is the standard deviation in FR from the statistical bootstrapping test. The lower confidence limit, taken as the avoidance threshold, was computed as $\mu-2\sigma$. When this lower threshold was below zero, then it was set to equal zero, meaning that the data is too sparse to differentiate avoidance from random behaviour. Any domains with an FR value within the upper and lower 95 % confidence interval thresholds was considered tolerated habitat, perhaps indicative of diverse life history choices but indistinguishable from random.

Given the FR value of each habitat quality class and its bootstrapped 95% statistical confidence limits, the final metric computed was the amount by which each observed FR for a bin stood out

beyond the limits for that bin, which was termed the FR residual (i.e. signal above noise). If the FR value for a bin fell between the avoidance and preference threshold values for that bin, then that location was assigned an FR residual value of 0, as it was indistinguishable from random selection and thus was considered tolerated habitat. If the residual was outside the thresholds, then the computation was conditional on whether the FR value was above or below one. In the former case, the preference threshold value was subtracted from the FR value. In the latter case, the avoidance threshold was subtracted from the FR value. The resulting scale for FR residuals is therefore centered on zero, with positive values indicating confident preference and negative values indicating confident avoidance. Using FR residuals effectively removes statistical uncertainty from the FR bioverification analysis, showing only the statistically significant habitat selection results for each habitat quality class. The use of 2σ is commonly considered a conservative standard, more likely to remove real information to ensure high confidence.

4.2.3 FR Test Bioverification Performance Indicators

The FR residuals test of a physical habitat model was required to meet two performance indicators in order for the model to be bioverified and therefore considered a successful model of physical microhabitat for *O. mykiss* spawning in the lower Yuba River. First, one or more habitat quality classes must be preferred and one or more avoided, as indicated by its FR residual. This establishes a significantly more rigorous standard than the Mann-Whitney U test, in that a physical habitat model must predict areas of both preference and avoidance (and do so beyond a 95% statistical significance), otherwise it provides only a trivial prediction. Second, because habitat quality classes inherently have a logical order, FR residuals must respect that order. Therefore, for a physical habitat model to be valid, FR residuals must be higher for habitat quality classes that represent higher quality habitat. The trend in FR residuals from low to high

quality habitat bins across all bioverification datasets may be interpreted to decide whether the number of bins should be increased or decreased and the analysis re-done on the new binning, depending on the needs for river management purposes. Thus, this procedure provides the scientific community with a test of the expert-based selection of the number and range of HSI bins, and the distinct levels of habitat quality they represent. A more detailed discussion of the bioverification performance indicators is available in Kammel & Pasternack (2014).

4.3 Habitat-Discharge Relationship

The bioverified physical habitat model was then used to quantify the area of available spawning habitat across a range of discharges using the concept of weighted usable area (WUA). WUA is the dominant statistical metric used in instream flow studies to represent the abundance of physical habitat available at a specific discharge based on statistical sampling (Bovee et al. 1998; Payne 2003). While past studies have equated WUA with an actual area (Bovee 1978; Stalnaker et al. 1995), others have argued WUA should be considered an index of habitat availability, as WUA studies have traditionally relied upon transect-based sampling of habitat availability (Williamson et al. 1993). This study is not a sampling, but a spatial census of habitat availability at 1-m resolution, so WUA can be interpreted more literally than with small sampled datasets. Also, other near-census measures of preferred habitat area can be computed besides WUA, especially drawing on the FR residuals bioverification test, but those options are beyond the scope of this study and yield similar results.

The WUA value in each raster cell was calculated by multiplying the CHSI value in each raster cell by the area of the cell (0.914 x 0.914 m^2). The sum of the WUA values from all raster cells within the wetted area at a single discharge provided a quantity of available spawning habitat at that discharge for *O. mykiss* spawning. After determining the WUA values across a range of

discharges, these values were plotted against discharge to produce a WUA-discharge relationship that illustrates the functional relationship between discharge and physical microhabitat availability (Bovee et al. 1998). WUA was calculated at discharges ranging from 8.5 to 141.6 m^3/s from the habitat suitability predictions of the CHSI physical habitat models. Cells with vegetation greater than 0.61 m tall (as determined by airborne LiDAR) were excluded from the calculation of available spawning habitat, as *O. mykiss* cannot spawn in areas with well-established vegetation. At a discharge of 28.3 m^3/s, more than 4% of the wetted area has woody vegetative cover, and therefore the vegetated areas were excluded from the WUA calculations at discharges greater than or equal to 28.3 m^3/s. For flows < 28.3 m^3/s, the percent wetted area that is vegetated is insignificant and therefore the vegetated areas were not exclused from the WUA calculations.

5 Results

5.1 Physical habitat model bioverification

Results of the Mann-Whitney U test of the physical habitat model at three discharges show that the CHSI model was bioverified according to this metric (Fig. 4). There are strong statistically significant differences ($p<0.002$) between the habitat quality at locations utilized for spawning and the habitat quality at randomly distributed, non-utilized points at all three discharges tested. In order of increasing discharge, the mean non-utilized CHSI values were 0.30, 0.28, and 0.24, while those for utilized locations were 0.70, 0.70, and 0.48, respectively. Thus, CHSI values differed by more than a factor of two between utilized and non-utilized spawning areas. The strong differentiation in quality between utilized and non-utilized locations in terms of statistical significance and mean CHSI values show that the CHSI physical habitat model was successful at

distinguishing *O. mykiss* spawning habitat based on the suitability of hydraulic and substrate conditions at the microhabitat scale.

The results of the FR test for the CHSI model were similar at the three discharges tested and showed a consistent increase in FR with increasing habitat quality (Fig. 5). For the intermediate habitat quality classes, it was found that at Q_{low} and Q_{mid} there was a secular increase in FR, which is ideal, while at Q_{high} the FR values decrease from habitat quality class 0.001-0.2 to 0.4-0.6. However, this should not be overinterpreted prior to FR residual analysis given how close both FR values were to one.

The results of the statistical bootstrapping analysis, and resulting preference and avoidance threshold values, show variability across the habitat quality classes and across the three discharges (Table 3). This is typical for such modest numbers of data points when a rare species is under investigation. For some habitat quality classes, such as 0.2-0.4 at Q_{low} and 0.8-1 Q_{mid}, it was effectively impossible to see avoidance of the habitat quality class because the avoidance threshold goes to zero by chance alone. The wide 95 % confidence intervals for these habitat quality classes are a result of small sample sizes and large standard deviation, meaning only very large deviations from a FR value of 1 would be indicative of preference or avoidance of habitat. Other habitat quality classes have a much narrower range of FR thresholds that indicate tolerated habitat, such as 0.6-0.8 at Q_{low} and 0.8-1 at Q_{high}. The lowest habitat quality class of 0-0.001 at each discharge has the smallest standard deviation and therefore the most narrow 95 % confidence interval because the habitat quality class represents a much smaller range of HSI values. The 95% confidence intervals were generally wider towards the extremes of highest (0.8-1) and lowest (0.001-0.2, excluding the assymetrical 0-0.001 habitat quality class) habitat quality. The standard deviations in FR at Q_{high} are generally smaller, due to the larger sample

size, and hence FR values that are relatively closer to one indicate greater preference and avoidance of habitat quality classes compared to the same FR value for lower discharges.

The FR residuals plot indicated that both of the performance indicators for bioverification were met at the three discharges, as there was one or more habitat quality classes avoided and one or more habitat quality classes preferred for spawning, and preference was shown for high-quality habitat classes, while avoidance was shown for the lower habitat quality classes (Fig. 6). At Q_{low} and Q_{mid}, the 0-0.001 and 0.001-0.2 habitat quality classes were avoided, while at Q_{high} only the lowest habitat quality class was avoided. The two highest quality habitat classes of 0.6-0.8 and 0.8-1.0 were preferred for spawning at the three discharges tested. The decrease in FR values from the 0.001-0.2 to 0.4-0.6 habitat quality classes observed at Q_{high} in Figure 5 was found to not violate bioverification because the utilization of the intermediate habitat quality classes was found to be indistinguishable from random, as evidenced by the FR residual value of 0 for these classes.

The FR residual results do not show any discharge-dependent change in spawning site selection over this flow range. While there was a decrease in the FR residuals in the 0.8-1 habitat quality class as discharge increased, this highest habitat quality class was still strongly preferred over the others – *O. mykiss* were three to four times more likely than random chance to select areas in the highest habitat quality class to spawn. Furthermore, the decrease in FR residuals for the highest quality class from 28.3 to 36.8 m^3/s was not matched by a similar magnitude increase in that metric for the 0–0.6 habitat quality classes.. It is also notable that the 0.6-0.8 habitat quality class did not show the opposite trend with discharge, which would have suggested that fish shifted down one class in habitat quality as flow increased. A similar effect like that with incremental shifting of utilization from one bin to the next was reported by Elkins et al. (2007), so it provides

552 a guide for how such a dependence would reveal itself in an analysis of an electivity index. The
553 apparent effect for the highest quality habitat bin seems more related to variability in the
554 bootstrapping thresholds. Thus the bioverified physical habitat model and conditions used by the
555 fish were discharge-independent across this range of discharges.

556 The hydraulic and substrate conditions within the preferred habitat quality classes of 0.6-1
557 represent the microhabitat conditions that are preferred for *O. mykiss* spawning in the Lower
558 Yuba River. According to the physical habitat model, there was a strong preference for spawning
559 in areas with a mean column velocity around 0.36-0.69 m/s, water depths of 0.38-0.84 m, and
560 mean substrate size from 32-90 mm, with slightly lower preference for mean substrate size from
561 90-200 mm. The physical habitat model correctly identified 46-67% of redds from the three redd
562 groups as located within preferred microhabitat (Table 4). The remaining 33-54% of individual
563 *O. mykiss* spawning location could not be predicted accurately within ~1 m based on
564 microhabitat suitability of hydraulics and substrate size alone. Of the redds not located within
565 preferred habitat, many of them were located within 1.5 m of preferred microhabitat. With the
566 addition of a 1.5 m buffer around areas of preferred microhabitat, 55-88% of redds across the
567 three redd groups were located within or very near preferred habitat areas. The physical habitat
568 model was bioverified at three discharges, and can be used not only to predict areas of high-
569 quality microhabitat for spawning, but also to quantify the availability of spawning habitat in the
570 lower Yuba River.

571

572 **5.2 Example Sites**

573 The full set of CHSI bioverification maps spanning 35.2 km with observed redds overlain for
574 each flow is too big to show in the article and thus is provided in the Supplementary Materials.
575 Microhabitat prediction performance is illustrated with three example sites, one for each flow
576 group, choosing sites with relatively large numbers of redds (Fig. 7). In all examples the majority
577 of redds was observed in the 0.8-1.0 CHSI bin, and no redds were observed in the 0.0-0.001 or
578 0.001-0.2 CHSI bins. There were also large areas of nonhabitat (CHSI=0-0.001) and relatively
579 small areas of highest quality habitat (CHSI=0.8-1.0) in the river. These results illustrate that the
580 predictions of preferred habitat were specific and constrained, providing a fairly precise model of
581 areas and physical habitat conditions expected to be utilized for spawning. Each example site
582 exhibited one large microhabitat patch with a CHSI of 0.8-1.0 along with one to two small
583 patches, with spawner preference apparently for the large patch. Within the example large
584 patches, redds were not preferentially located at the patch entrance or exit, which suggests there
585 is no local control by hyporheic conditions. All of the highest quality habitat patches in the
586 example sites were closer to the bank than the center of the river, but the spawners were not
587 disproportionately aligned along the bank. These results illustrate the outcome of many such tests
588 that found that among the diverse possible microhabitat factors, depth, velocity, and substrate
589 were the dominate controls on redd location. Finer spatial differences in redd location appear
590 random.

591 **5.3 Habitat-Discharge Relationship**

592 The bioverified CHSI model was used to compute habitat area across a range of in-channel
593 discharges from 8.5 to 141.6 m^3/s. (Fig. 8). The maximum habitat area was found at 17.61 m^3/s.

At this flow there was 67.3 ha of habitat. Above 24.9 m^3/s, habitat area quickly decreased and stabilized to a fairly constant minimum value up to the bankfull discharge.

6 Discussion

6.1 Physical Habitat Model Bioverification

The physical habitat model provided a comprehensive and quantitative understanding of the physical microhabitat conditions that are preferred for spawning of the rare, elusive species *O. mykiss*. It also was found to be predictive of spawning habitat utilization. The utilization-based hydraulic HSCs that were site-specific to the lower Yuba River provided a successful physical habitat model, along with a substrate HSC that was a blend of data-driven and expert-guided elements after analysis of 12 alternatives. The physical habitat model using these HSCs was fairly restrictive and precise— limiting the amount of wetted area that was assigned high suitability— resulting in strong preference for high-quality habitat according to the FR test. The physical habitat model was bioverified at three discharges, showing that the microhabitat conditions preferred for *O. mykiss* spawning are consistent throughout the range of discharges tested in this study. It would be beneficial in the future to be able to test the discharge-independence of the physical habitat model with spawning observations across a wider range of discharges than was possible given the hydroclimate during the years of this study to evaluate whether the microhabitat hydraulic and substrate conditions preferred by *O. mykiss* spawners really do not change.

Habitat suitability modelling for salmonids and other fish has progressed rapidly in recent years with advancements in remote sensing, 2D modelling, and spatial and 3D tools in GIS (Pasternack & Senter 2011; Maddock et al. 2013). This study of *O. mykiss* spawning habitat used a

traditional approach of physical habitat modelling through the assessment of habitat suitability with HSCs applied to near-census datasets and 2D hydrodynamic model outputs. This facilitated the representation of hydraulic and substrate conditions in the river at a much finer resolution and on a larger scale compared to traditional transect-based sampling or the use of 1D model results. The resulting physical habitat model was spatially explicit, of high resolution, and predictive of habitat quality and quantity across a range of discharges up to bankfull. Near-census physical habitat models made it possible to accurately quantify the amount of spawning habitat available in the lower Yuba River without the experimental design sacrifices and trade-offs required of a sampling methodology, which is beneficial in developing WUA-discharge relationships of habitat availability. Ongoing rapid improvements to bathymetric remote sensing will improve model performance and expand the scope of streams accessible for near-census assessment.

One of the most innovative methodological aspects of this study was the application of statistical bootstrapping tests to provide a measure of statistical significance to the FR test results, which is especially important with small populations yet has hardly been done in modern ecohydraulics. The addition of the bootstrapping test in conjunction with the FR test provides a 95% confidence interval around FR=1 for the preferences and avoidances interpreted from the test, rather than depending on the simple FR>1 for preferred domains and FR<1 for avoided domains that has been used to interpret FR test results in past studies (e.g. Deudero & Morales-Nin 2001; Estep et al. 2011). This added level of statistical significance means the FR test results can be vetted to determine if they provide meaningful outcomes with regards to understanding the physical habitat preferences of rare species.

A large number of redds were located in close proximity to areas of preferred microhabitat. The spawning activity near areas designated as preferred spawning habitat may still be influenced by the suitable microhabitat conditions, but their location just outside of the preferred areas may result from the social behaviour of the fish to cluster around other spawners (Essington et al. 1998; Mull & Wilzbach 2007) or from small errors in the delineation of the habitat quality class patches, due to the propagation of uncertainty from the hydrodynamic model results and the substrate mapping efforts into the CHSI model results. Model performance at the meter scale was also potentially impacted by localized topographic changes during the time between river mapping in 2006 and the time span of the spawning surveys in 2010 and 2011. It may also have been impacted by winter flow fluctuations in the week between surveys. For the 12-45% of redds defying model predictions, individuals may have selected spawning locations based on habitat characteristics that were not captured by the modelling, including factors beyond the microhabitat scale. It is also possible that these individuals selected spawning sites based on random choices. Either way, this results in diverse life histories that may promote diversity and resilience in the population. Because the lower Yuba River contained hundreds of thousands of square meters of diverse and dynamic in-channel bed areas, there was ample opportunity for individuals to select spawning sites, but most importantly there was an abundance of unoccupied preferred microhabitat that was not used during each particular year. In any case, the river had an overabundance of both preferred habitat and diverse features to provide for the full range of *O. mykiss* spawning behaviour.

6.2 Habitat-Discharge Relationship

The amount of available high-quality spawning habitat was highly dependent on discharge, but even at very low or high in-channel flows, there was no lack of high-quality spawning habitat in

661 the lower Yuba River, with hundreds of thousands of square meters of preferred habitat available
662 to *O. mykiss* spawners. The lower Yuba River currently sustains a population of several hundred
663 *O. mykiss* spawners each year, but contains far more preferred microhabitat than is used by the
664 current population and is likely capable of sustaining several thousand spawners (Kammel &
665 Pasternack 2014). While there is abundant high-quality spawning habitat available in the lower
666 Yuba River for *O. mykiss* spawners, this cannot offset the myriad factors impacting each
667 lifestage that have caused the anadromous *O. mykiss* population to have been nearly extirpated
668 from its historical range in the Central Valley, including the loss and degradation of freshwater
669 habitat, predation and migratory losses, alteration of natural flow regimes, unsustainable and
670 inadequate rearing habitat, and impassable barriers, among many others (NMFS 2014).

671 Past studies have argued for the use of WUA values as an index of the relative abundance of
672 physical habitat rather than a specified quantity of available habitat, because WUA was
673 traditionally calculated from a statistical sampling of transects (or discrete sampled areas) within
674 the river, rather than from the habitat suitability of the entire wetted area (Williamson et al. 1993;
675 Payne 2003). In this study, the high spatial resolution of the 2D hydrodynamic and physical
676 habitat models allowed for accurate quantification of available area, making the WUA values
677 explicit quantities of available habitat area at each discharge, rather than the relative metric it has
678 been used for in the past when available area could not be accurately quantified.

679 The WUA-discharge relationship for *O. mykiss* spawning provides a useful tool for the
680 optimization of flows during the spawning season in order to provide the abundant high-quality
681 habitat , although it is evident that all flows provide far more habitat than the current population
682 size can use. Instream flow optimization is a difficult river management task, as the needs of all
683 species should be considered to provide adequate habitat during sensitive life stages and at

684 critical times of the year, as well as the obligation to balance the biological needs with societal
685 needs of water supply and hydropower production. In the lower Yuba River, the optimal flows to
686 provide the most habitat for spawning *O. mykiss* and those for spawning Chinook salmon are
687 very similar, with a peak discharge from the WUA-discharge relationship for Chinook salmon
688 spawning at about 17 m^3/s (Pasternack et al. 2014). This method of physical habitat modelling
689 with high-resolution datasets and 2D hydrodynamic model results can be conducted for any
690 number of species and lifestages of interest, making it possible to more accurately quantify
691 physical habitat availability for the organisms of interest and optimize the flows in regulated
692 rivers to meet their needs throughout the year.

693 ## 7 Conclusions

694 The bioverified physical habitat model shows that there is a specific range of hydraulic and
695 substrate conditions at the microhabitat scale that are preferred by *O. mykiss* spawners in the
696 lower Yuba River. *O. mykiss* spawning habitat use was highly predictable, with a large fraction
697 of observed spawning sites located in areas predicted to be preferred microhabitat according to
698 the physical habitat model. The suitability of microhabitat conditions explains the location of
699 much of the observed spawning activity, but alone cannot capture all of the variability of
700 spawning site locations. There are likely factors beyond the microhabitat scale that influence *O.*
701 *mykiss* spawning site selection. Preferred microhabitat conditions based on water depth, velocity,
702 and substrate size are abundantly available to spawners in the lower Yuba River, so access to
703 high-quality spawning habitat is not a limiting factor on *O. mykiss* spawning success in the river.

704 The predictive physical habitat model produced in this study provides not only the means to
705 characterize and identify areas of high-quality microhabitat for *O. mykiss* spawning, but also a

706 way to quantify available habitat across a range of discharges and evaluate the impact of
707 different flow regimes on the availability of *O. mykiss* spawning habitat in the regulated lower
708 Yuba River. The development of physical habitat models at this scale and high spatial resolution
709 can be applied to other species and lifestages of interest, particularly rare populations that are not
710 reliably sampled with a traditional reach-based approach, to provide accurate and quantitative
711 measures of available habitat area to inform comprehensive instream flow assessments.

712

713 8 Acknowledgments

714 Primary support for this study was provided by the Yuba County Water Agency (Award
715 #201016094) and as in-kind aid from the Yuba Accord River Management Team. This project
716 was also supported by the USDA National Institute of Food and Agriculture, Hatch project
717 number #CA-D-LAW-7034-H. We thank Mathew Jian, Denise Tu, Joshua Wyrick, Bobby
718 Gonzalez, Casey Campos, Tom Johnson, Elizabeth Campbell, and Eugene Geary for various
719 assistance and feedback. Independent peer reviews by three reviewers and the associate editor
720 were helpful in improving the final manuscript for publication.

721

722

723 9 References

724 Abu-Aly, T.R., Pasternack, G.B., Wyrick, J. R., Barker, R., Massa, D., Johnson, T. 2013. Effects
725 of LiDAR-derided, spatially-distributed vegetative roughness on 2D hydraulics in a

726 gravel-cobble river at flows of 0.2 to 20 times bankfull. Geomorphology 206: 468–482.
727 doi:10.1016/j.geomorph.2013.10.017.

728 Anderson, M.G., Bates, P.D. 1994. Evaluating data constraints on two-dimensional finite
729 element models of floodplain flow. Catena 22: 1–15.

730 Annear, T.C., Conder, A.L. 1984. Relative Bias of Several Fisheries Instream Flow Methods. N.
731 Am. J. Fish. Manag. 4(4B):531-539.

732 Baldridge, J.E. 1981. Development of Habitat Suitability Criteria: Appendix 3. In: An
733 Assessment Of Environmental Effects of Construction And Operation of the Proposed
734 Terror Lake Hydroelectric Facility, Kodiac, Alaska (Eds. W.J. Wilson, E.W. Trihey, J.E.
735 Baldridge, C.D. Evans, J.G. Thiele, D.E. Trudgen), p. 357-419. Arctic Environmental
736 Information and Data Center, University of Alaska, Anchorage.

737 Barker, J.R. 2011. Rapid, abundant velocity observation to validate million-element 2D
738 hydrodynamic models [M.S. Thesis]. Davis (CA): University of California at Davis.

739 Beland, K.F., Jordan, R.M., Meister, A.L. 1982. Water depth and velocity preferences of
740 spawning Atlantic salmon in Maine rivers. N. Am. J. Fish. Manag. 2:11–13.

741 Bovee, K.D. 1978. Probability-of-use Criteria for the Family Salmonidae. Fort Collins (CO):
742 Cooperative Instream Flow Service Group, Instream Flow Information Paper 4.

743 Bovee, K.D. 1996. The Complete IFIM: A Coursebook for IF 250. Fort Collins (CO): U.S.
744 Geological Survey.

745 Bovee, K.D., Lamb, B.L., Bartholow, J.M., Stalnaker, C.B., Taylor, J., Henrikson, J. 1998.
746 Stream habitat analysis using the instream flow incremental methodology. U.S.
747 Geological Survey. (USGS/BRD-1998-0004).

748 Boydstun LB, McDonald T. 2005. Action plan for monitoring California's coastal Salmonids.
749 Santa Cruz (CA): Boydstun (NOAA Fisheries Contract Number WASC-3-1295).

750 Briggs, J.C. 1953. The Behaviour and Reproduction of Salmonid Fishes in a Small Coastal
751 Stream. Stanford (CA): State of California Department of Fish and Game Marine
752 Fisheries Branch.

753 Burner, C.J. 1951. Characteristics of Spawning Nests of Columbia River Salmon. Washington,
754 D.C.: United States Fish and Wildlife Service.

755 Busby, P. J., Wainwright, T. C., Bryant, B. J., Lierheimer, L. J., Waples, R. S., Waknitz, F. W.,
756 Lagomarsino, I. 1996. Status Review of West Coast Steelhead from Washington, Idaho,
757 Oregon, and California". NOAA Technical Memorandum. NMFS-NWFSC-27. P1-255
758 (255).

759 Campos C, Massa D. 2009. Appendix I. Specific sampling protocols and procedures for
760 conducting adult Chinook salmon and steelhead redd surveys-Yuba River Chinook
761 salmon and steelhead redd surveys. Marysville (CA): Yuba River Accord Management
762 Team.

763 Campos C, Massa D. 2011. Annual Redd Survey Report: August 31, 2009–April 8, 2010.
764 Marysville (CA): Yuba River Accord Management Team.

765 Campos C, Massa D. 2012. Annual Redd Survey Report: 2010–2011. Marysville (CA): Yuba
766 River Accord Management Team.

767 Carley, J. K., Pasternack, G. B., Wyrick, J. R., Barker, J. R., Bratovich, P. M., Massa, D. A.,
768 Reedy, G. D., Johnson, T. R. 2012. Significant decadal channel change 58-67 years post-
769 dam accounting for uncertainty in topographic change detection between contour maps
770 and point cloud models. Geomorphology 179: 71–88.
771 doi:10.1016/j.geomorph.2012.08.001.

772 Cederholm, C.J., Salo, E.O. 1979. The effects of logging road landslide siltation on the salmon
773 and trout spawning gravels of Stequaleho Creek and the Clearwater River Basin,
774 Jefferson County, Washington, 1972-1978. Seattle (WA): University of Washington,
775 Fishery Resource Institute.

776 Chambers, J.S., Pressey, R.T., Donaldson, J.R., McKinley, W.R. 1954. Research relating to
777 study of spawning grounds in natural areas, Annual Report. Olympia (WA): Department
778 of Fisheries, State of Washington. Contract DA 35026-Eng-20572.

779 Chambers, J.S., Allen, G.H., Pressey, R.T. 1955. Research relating to study of spawning grounds
780 in natural areas, Annual Report. Olympia (WA): Department of Fisheries, State of
781 Washington. Contract DA 35026-Eng-20572.

782 Crowder, D.W., Diplas, P. 2006. Applying spatial hydraulic principles to quantify stream habitat.
783 River Res. Appl. 22: 79-89.

784 Curtis, J.A., Flint, L.E., Alpers, C.N., Yarnell, S.M. 2005. Conceptual model of sediment
785 processes in the upper Yuba River watershed, Sierra Nevada, CA. Geomorphology.
786 68:149-166.

787 Deudero, S., Morales-Nin, B. 2001. Prey Selectivity in Planktinivorous Juvenile Fishes
788 Associated With Floating Objects in the Western Mediterranean. Aquac. Res. 32:481-
789 490.

790 Dixon, P.M. 1998. The bootstrap and the jackkinfe: Describing the precision of ecological
791 indices. In: Design and Analysis of Ecological Experiments (Eds. S.M. Scheiner, J.
792 Gurevitch), p. 290-318. New York (NY): Chapman & Hall.

793 Efron, B., Tibshirani, R. 1993. An Introduction to the Bootstrap. Boca Raton (FL): Chapman &
794 Hall/CRC.

795 Elkins, E.E., Pasternack, G.B., Merz, J.E. 2007. The Use of Slope Creation for Rehabilitating
796 Incised, Regulated, Gravel-Bed Rivers. Water Resour. Res. 43. W05432,
797 doi:10.1029/2006WR005159.

798 Essington, T.E., Sorenson, P.W., Paron, D. G. 1998. High rate of redd superimposition by brook
799 trout (*Salvelinus fontinalis*) and brown trout (*Salmo trutta*) in a Minnesota stream cannot
800 be explained by habitat availability alone. Can. J. of Fish. Aquat. Sci. 55:2310-2316.

801 Estep, L.K., McClure, C.J.W., Burkett-Cadena, N.D., Hassan, H.K., Hicks, T.L., Unnasch, T.R.,
802 Hill, G.E. 2011. A Multi-Year Study of Mosquito Feeding Patterns on Avian Hosts in a
803 Southeastern Focus of Eastern Equine Encephalitis Virus. Am. J. Trop. Med. Hyg.
804 84:718-726.

805 Gallagher, S.P., Hahn, P.J., Johnson, D.H. 2007. Redd Counts. In: Salmonid Field Protocols
806 Handbook: Techniques for Assessing Status and Trends in Salmon and Trout Populations
807 (Eds. D.H. Johnson, B.M. Shrier, J.S. O'Neal, J.A. Knutzen, X. Augerot, T.A. O'Neil,
808 T.N. Pearsons), p. 197-234. American Fisheries Society, Bethesda., MD.

809 Geist, D.R., Dauble, D.D. 1998. Redd site selection and spawning habitat use by fall Chinook
810 salmon: the importance of geomorphic features in large rivers. Environ. Manag. 22:655–
811 669.

812 Gilbert, G.K. 1917. Hydraulic-mining debris in the Sierra Nevada. Washington, D.C.: U.S.
813 Geological Survey.

814 Gonzalez, R.L., Pasternack, G.B. 2015. Re-envisioning cross-sectional hydraulic geometry as
815 spatially explicit hydraulic topography. Geomorphology. 246:394–406.

816 Good, T.P., Waples, R.S., Adams, P. 2005. Updated status of federally Listed ESUs of West
817 Coast salmon and steelhead. U.S. Department of Commerce.

818 Hanrahan, T.P. 2007. Bedform morphology of salmon spawning areas in a large gravel-bed river.
819 Geomorphology. 86:529–536.

820 Hess, A.D., Swartz, A. 1940. The forage ratio and its use in determining the food grade of
821 streams. Trans. N. Am. Wildl. Conf. 5:162-164.

822 Ivlev, V.S. 1961. Experimental ecology of the feeding of fishes. New Haven (CT): Yale
823 University Press.

824 Jackson, J.R., Pasternack, G.B., Wyrick, J.R. 2013. Substrate of the Lower Yuba River. Davis
825 (CA): Prepared for the Yuba Accord River Management Team. University of California
826 at Davis.

827 James, L.A., Singer, M.B., Ghoshal, S., Megison, M. 2009. Historical channel changes in the
828 lower Yuba and Feather Rivers, California: Long-term Effects of Contrasting River-
829 Management Strategies. In: Management and Restoration of Fluvial Systems with Broad
830 Historical Changes and Human Impacts (Eds. L.A. James, S.L. Rathburn, G.R.
831 Whittecar), p. 57-81. Geological Society of America Special Paper 451.

832 Johnson, D.H. 1980. The comparison of usage and availability measurements for evaluating
833 resource preference. Ecology. 61:65-71.

834 Kammel, L. Pasternack, G. B. 2014. *O. mykiss* adult spawning physical habitat in the lower Yuba
835 River. Davis (CA): Prepared for the Yuba Accord River Management Team. University
836 of California at Davis.

837 Kobayashi, D.R., Polovina, J.J., Parker, D.M., Kamezaki, N., Cheng, I.J., Uchida, I., Dutton,
838 P.H., Balazs, G.H. 2008. Pelagic habitat characterization of loggerhead sea turtles,
839 *Caretta caretta*, in the North Pacific Ocean (1997-2006): Insights from satellite tag
840 tracking and remotely sensed data. J. Exp. Mar. Biol. Ecol. 356:96-114.

841 Kondolf, G.M., Wolman, M.G. 1993. The Sizes of Salmonid Spawning Gravels. Water Resour.
842 Res. 29:11.

843 Kozlowski, J.F. 2004. Summer Distribution, Abundance, and Movements of Rainbow Trout
844 (*Oncorhynchus mykiss*) and other Fishes in the Lower Yuba River, California [M.S.
845 Thesis]. Davis (CA): University of California at Davis.

846 Lai, Y.G. 2008. SRH-2D Version 2: Theory and User's Manual. Denver (CO): U.S. Department
847 of the Interior, Bureau of Reclamation, Technical Service Center.

848 Lechowicz, M.J. 1982. The Sampling Characteristics of Electivity Indices. Oecologia (Berl).
849 52:22-30.

850 Leclerc, M., Boudreault, A., Bechara, J., Corfa, G. 1995. Two-dimensional Hydrodynamic
851 Modelling: A Neglected Tool in the Instream Flow Incremental Methodology. Trans.
852 Am. Fish. Soc. 124:645-662.

853 Lindley, S.T., Schick, R.S., Agrawal, A., Goslin, M., Pearson, T.E., Mora, E., Anderson, J.J.,
854 May, B., Greene, S., Hanson, C., Low, A., McEwan, D., MacFarlane, R.B., Swanson, C.,
855 Williams, J.G. 2006. Historical population structure of Central Valley steelhead and its
856 alteration by dams. San Franc. Estuary Watershed Sci., John Muir Institute of the
857 Environment, UC Davis. 4.

858 Maddock, I., Kemp, P., Harby, A., eds. 2013. Ecohydraulics: an integrated approach. Chichester:
859 Wiley and Sons.

860 Mann, H.B., Whitney, D.R. 1947. On a test of whether one of two random variables is
861 stochastically larger than the other. Ann. Math. Stat. 18.

862 Massa, D., Bergman, J., Greathouse, R. 2012. Annual Vaki Riverwatcher Report: March 1,
863 2009-February 28, 2010. Lower Yuba River Accord Monitoring and Evaluation Plan.

864 McEwan, D.R. 2001. Central Valley Steelhead. In: Fish Bulletin 179. Contributions to the
865 biology of Central Valley salmonids (Ed. R.L. Brown). Sacramento (CA): California
866 Department of Fish and Game.

867 Merz, J.E., Setka, J.D. 2004. Evaluation of a Spawning Habitat Enhancement Site for Chinook
868 Salmon in a Regulated California River. N. Am. J. Fish. Manag. 24:397-407.

869 Mitchell, W.T. 2010. Age, Growth, and Life History of Steelhead Rainbow Trout (*Oncorhynchus*
870 *mykiss*) in the Lower Yuba River, California. ICF International, March 2010.

871 Moir, H.J., Pasternack, G.B. 2008. Relationships between mesoscale morphological units, stream
872 hydraulics and Chinook salmon (*Oncorhynchus tshawytscha*) spawning habitat on the
873 Lower Yuba River, California. Geomorphology. 100:527-548.

874 Moir, H.J., Pasternack, G.B. 2010. Substrate requirements of spawning Chinook salmon
875 (*Oncorhynchus tshawytscha*) are dependent on local channel hydraulics. River Res. Appl.
876 26:456-468.

877 Mull, K.E., Wilzbach, M.A. 2007. Selection of spawning sites by coho salmon in a northern
878 California stream. N. Am. J. Fish. Manag. 27:343-1354.

879 [NMFS] National Marine Fisheries Service 2009. Public Draft Recovery Plan for the
880 Evolutionarily Significant Units of Sacramento River Winter-run Chinook Salmon and
881 Central Valley Spring-run Chinook Salmon and the Distinct Population Segment of

Central Valley Steelhead. Sacramento (CA): NMFS Sacramento Protected Resources Division.

[NMFS] National Marine Fisheries Service 2014. Recovery Plan for the Evolutionarily Significant Units of Sacramento River Winter-run Chinook Salmon and Central Valley Spring-run Chinook Salmon and the Distinct Population Segment of California Central Valley Steelhead. Sacramento (CA): NMFS Sacramento Protected Resources Division.

Noack, M., Schneider, M., Wieprecht, S. 2013. The Habitat Modelling System CASiMiR: A Multivariate Fuzzy Approach and its Applications. In: Ecohydraulics: an integrated approach (Eds. Maddock, I., Harby, A., Kemp, P., Wood, P.). Chichester (UK): John Wiley & Sons, Ltd.

Orcutt, D., Pulliam, B., Arp, A. 1968. Characteristics of steelhead trout redds in Idaho streams. Trans. Am. Fish. Soc. 97:42-45.

Parasiewicz, P. and Walker, J.D. 2007. Comparison of MesoHABSIM with two microhabitat models (PHABSIM and HARPHA). River Res. Appl. 23**:**904–923. doi: 10.1002/rra.1043.

Pasternack, G.B. 2009. Specific Sampling Protocols and Procedures for Topographic Mapping. Marysville (CA): The Lower Yuba River Accord Planning Team.

Pasternack, G.B. 2011. 2D Modelling and Ecohydraulic Analysis. Seattle (WA): Createspace.

Pasternack, G.B., Senter, A.E. 2011. 21st Century instream flow assessment framework for mountain streams. California Energy Commission, PIER.

902 Pasternack, G.B., Tu, D., Wyrick, J.R. 2014. Chinook Adult Salmon Spawning Physical Habitat
903 of the Lower Yuba River, Final Report. Davis (CA): Lower Yuba River Accord
904 Monitoring and Evaluation Program.

905 Pasternack, G.B., Gilbert, A.T., Wheaton, J.M., Buckland, E.M. 2006. Error Propagation for
906 Velocity and Shear Stress Prediction Using 2D Models For Environmental Management.
907 J. Hydrol. 328:227-241.

908 Payne, T.R. 2003. The Concept of Weighted Usable Area as Relative Suitability Index. IFIM
909 Users Workshop, 2003 June 1-5; Fort Collins, CO, 14 pp.

910 Sams, R.E., Pearson, L.S. 1963. A study to develop methods for determining spawning flows for
911 anadromous salmonids. Portland (OR): Oregon Fish Commission, 56 pp.

912 Savage, R.E. 1931. The relation between the feeding of the herring off the east coast of England
913 and the plankton of the surrounding waters. London (UK): Fishery Investigations,
914 Ministry of Agriculture, Food, and Fisheries. Series II, 12:1-88.

915 Shirazi, M.A., Seim, W.K. 1981. Stream System Evaluation with Emphasis on Spawning Habitat
916 for Salmonids. Water Resourc. Res. 17:592-594.

917 Shorygin, A.A. 1939. Foods, selective capacity and food interrelationships of certain *gobiidae* of
918 the Caspian Sea. Zoologichesky Zhurnal. 18:27-53.

919 Smith, A.K. 1973. Development and Application of Spawning Velocity and Depth Criteria for
920 Oregon Salmonids. Trans. Am. Fish. Soc. 102:312-316.

Stalnaker, C.B, Lamb, B.L., Henriksen, J., Bovee, K., Bartholow, J. 1995. The Instream Flow Incremental Methodology: a primer for IFIM. Biological Report 29. Fort Collins (CO): United States National Biological Service.

Swift, C.H. 1976. Estimation of Stream Discharges Preferred by Steelhead Trout for Spawning and Rearing in Western Washington. Tacoma (WA): United States Geological Survey.

Thomson, J.R., Taylor, M.P., Brierley, G.J., 2004. Are River Styles ecologically meaningful? A test of the ecological significance of a geomorphic river characterization scheme. Aquat. Conserv. 14:25-48.

[USFWS] United States Fish and Wildlife Service. 1996. Identification of the Instream Flow Requirements for Steelhead and Fall-run Chinook Salmon Spawning in the Lower American River. Sacramento (CA).

[USFWS] United States Fish and Wildlife Service. 1997. Microhabitat Suitability Criteria for Anadromous Salmonids of the Trinity River. Arcata (CA).

[USFWS] United States Fish and Wildlife Service. 2007. Flow-Habitat Relationships for Spring-run Chinook Salmon and Steelhead/Rainbow Trout Spawning in Clear Creek Between Whiskeytown Dam and Clear Creek Road. Sacramento (CA).

Vondracek, B., Longanecker, D.R. 1993. Habitat Selection By Rainbow Trout, *Oncorhynchus mykiss*, in a California Stream: Implications for the Instream Flow Incremental Methodology. Ecol. of Freshw. Fish. 2:173-186.

940 Williams, C.S., Marshall, W.H. 1938. Duck nesting studies, Bear River Migratory Bird Refuge,
941 Utah, 1937. J. Wildl. Manag. 2:29-48.

942 Williamson, S.C., Bathrolow, J.M., Stalnaker, C.B. 1993. Conceptual model for quantifying pre-
943 smolt production from flow-dependent physical habitat and water temperature. Regul.
944 Rivers: Res. Manag. 8:15-28.

945 Wyrick, J.R., Pasternack, G.B. 2012. Landforms of the Lower Yuba River. Davis (CA): Lower
946 Yuba River Accord Monitoring and Evaluation Program.

947 Wyrick, J.R., Pasternack, G.B. 2014. Geospatial organization of fluvial landforms in a gravel-
948 cobble river: beyond the riffle-pool couplet. Geomorphology. 213**:**48-65.
949 doi:10.1016/j.geomorph.2013.12.040.

950 Wyrick, J.R., Pasternack, G.B. 2015. Revealing the natural complexity of topographic change
951 processes through repeat surveys and decision-tree classification. Earth Surf. Process.
952 Landforms. doi: 10.1002/esp.3854

953 [YARMT] Yuba Accord River Management Team. 2013. Lower Yuba River accord, river
954 management team interim monitoring and evaluation report (draft). Marysville (CA):
955 Yuba River Accord River Management Team.

956 Zimmerman, C.E., Edwards, G.W., Perry, K. 2009. Maternal Origin and Migratory History of
957 Steelhead and Rainbow Trout Captured in Rivers of the Central Valley, California. Trans.
958 Am. Fish. Soc. 138:280-291.

Table 1. Observed and modeled flows for *O. mykiss* redd groups.

Redd group	# redds	2D model discharge (m^3/s)	Range of observed discharges in the group [average discharge] (m^3/s)
Q_{low}	43	24.9	24.24 - 24.27 [24.24]
Q_{mid}	54	28.3	27.18 - 29.73 [28.46]
Q_{high}	94	36.8	35.68 - 37.09 [36.03]

959

960

961

962

Table 2. Habitat suitability index bin delineations and habitat quality class descriptions.

Combined Habitat Suitability Index Bin	Habitat Quality Class
$0 \leq CHSI < 0.001$	Non-habitat
$0.001 \leq CHSI < 0.2$	Poor quality habitat
$0.2 \leq CHSI < 0.4$	Low quality habitat
$0.4 \leq CHSI < 0.6$	Medium quality habitat
$0.6 \leq CHSI < 0.8$	High quality habitat
$0.8 \leq CHSI < 1.0$	Highest quality habitat

963

964

Table 3. Statistical bootstrapping results (among 10 random datasets with the same number of points as the real data.) and the resulting 95 % confidence intervals to obtain preference and avoidance thresholds.

Redd group	Habitat Quality Class	Mean Forage Ratio	Standard Deviation	Avoidance Threshold	Preference Threshold
Q_{low}	0 - 0.001	0.93	0.08	0.77	1.08
	0.001 - 0.2	1.31	0.51	0.29	2.33
	0.2 - 0.4	1.04	0.53	-0.01	2.10
	0.4 - 0.6	0.89	0.26	0.36	1.41
	0.6 - 0.8	0.93	0.22	0.48	1.38
	0.8 - 1	1.19	0.41	0.37	2.02
Q_{mid}	0 - 0.001	0.90	0.13	0.64	1.15
	0.001 - 0.2	1.62	0.34	0.95	2.30
	0.2 - 0.4	1.01	0.31	0.38	1.63
	0.4 - 0.6	0.95	0.42	0.12	1.79
	0.6 - 0.8	1.05	0.37	0.30	1.80
	0.8 - 1	0.93	0.47	0.00	1.86
Q_{high}	0 - 0.001	0.98	0.09	0.81	1.15
	0.001 - 0.2	1.16	0.28	0.60	1.71
	0.2 - 0.4	0.95	0.26	0.43	1.47
	0.4 - 0.6	1.14	0.38	0.39	1.90
	0.6 - 0.8	0.95	0.40	0.15	1.75
	0.8 - 1	0.87	0.27	0.34	1.40

965

966

967

968

Table 4. Microhabitat prediction performance results.

Redd group	# redds	% in preferred microhabitat	% in or within 1.5 m of preferred microhabitat
Q_{low}	43	67	88
Q_{mid}	54	67	81
Q_{high}	94	46	55

969

970

971 **Figure Captions**

972

973 Figure 1. Location map of the lower Yuba River.

974 Figure 2. Experimental design schematic for bioverification using a new forage ratio method.
975 Light grey fill indicates data and model inputs. Dark grey diamonds indicate scientific test
976 decision points.

977 Figure 3. Local habitat suitability curves for *O. mykiss* spawning adults.

978 Figure 4. Mann-Whitney U Test results comparing habitat quality of utilized and non-utilized
979 locations at the three discharges tested.

980 Figure 5. Forage ratio test results for the physical habitat model.

981 Figure 6. Forage ratio residuals results for the physical habitat model showing statistically
982 significant preferences and avoidances beyond the 95% confidence level.

983 Figure 7. Habitat quality maps for three sites, one for each discharge. The dot size for each redd
984 is not to scale, but was enlarged to aid visibility on the maps.

985 Figure 8. WUA-discharge relationship for spawning *O. mykiss*.

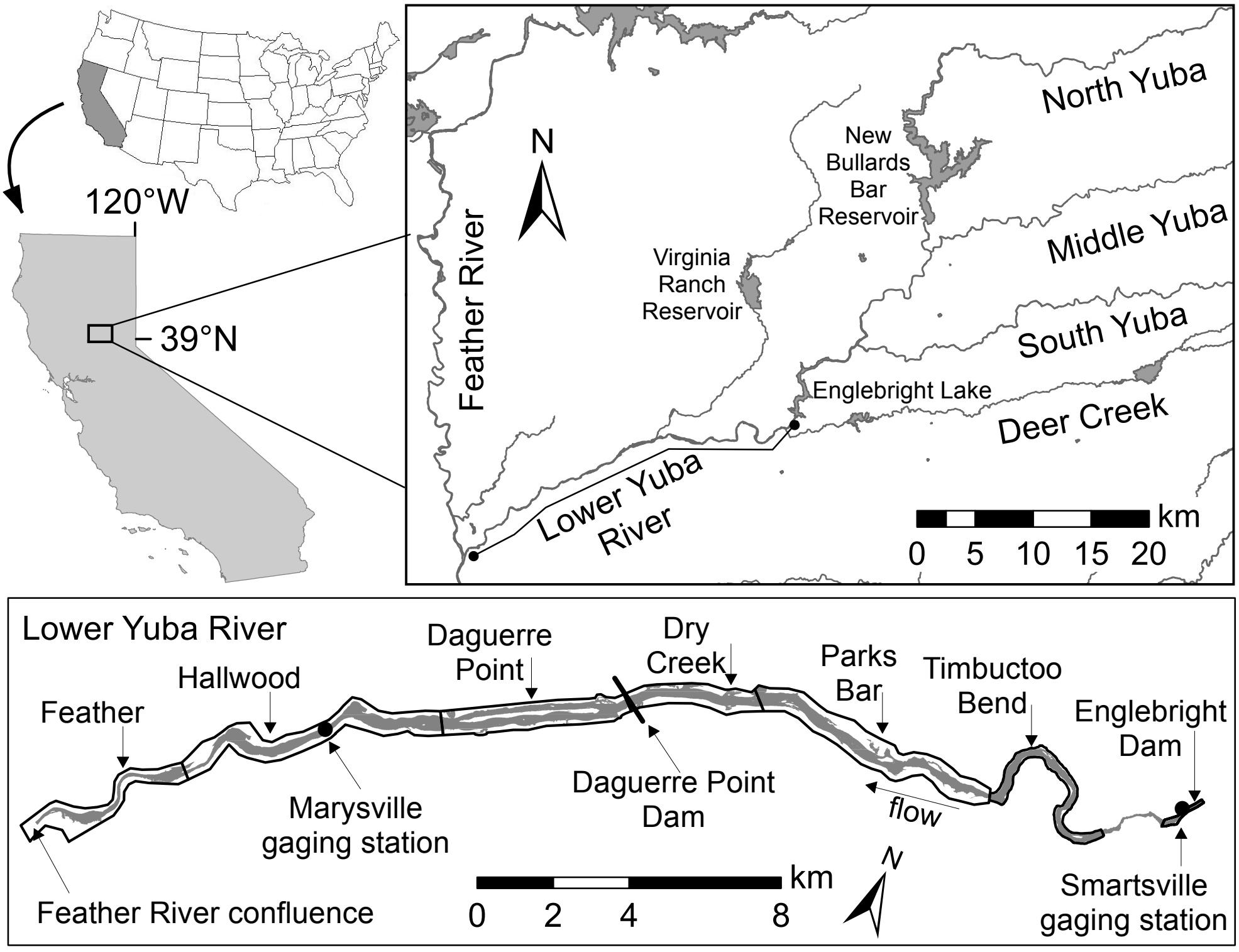
120°W
39°N
N
Feather River
New
Bullards
Bar
Reservoir
Virginia
Ranch
Reservoir
North Yuba
Middle Yuba
South Yuba
Englebright Lake
Deer Creek
Lower Yuba
River
km
0 5 10 15 20
Lower Yuba River
Feather
Hallwood
Marysville
gaging station
Daguerre
Point
Dry
Creek
Daguerre Point
Dam
Parks
Bar
Timbuctoo
Bend
flow
Englebright
Dam
Smartsville
gaging station
Feather River confluence
km
0 2 4 8
N

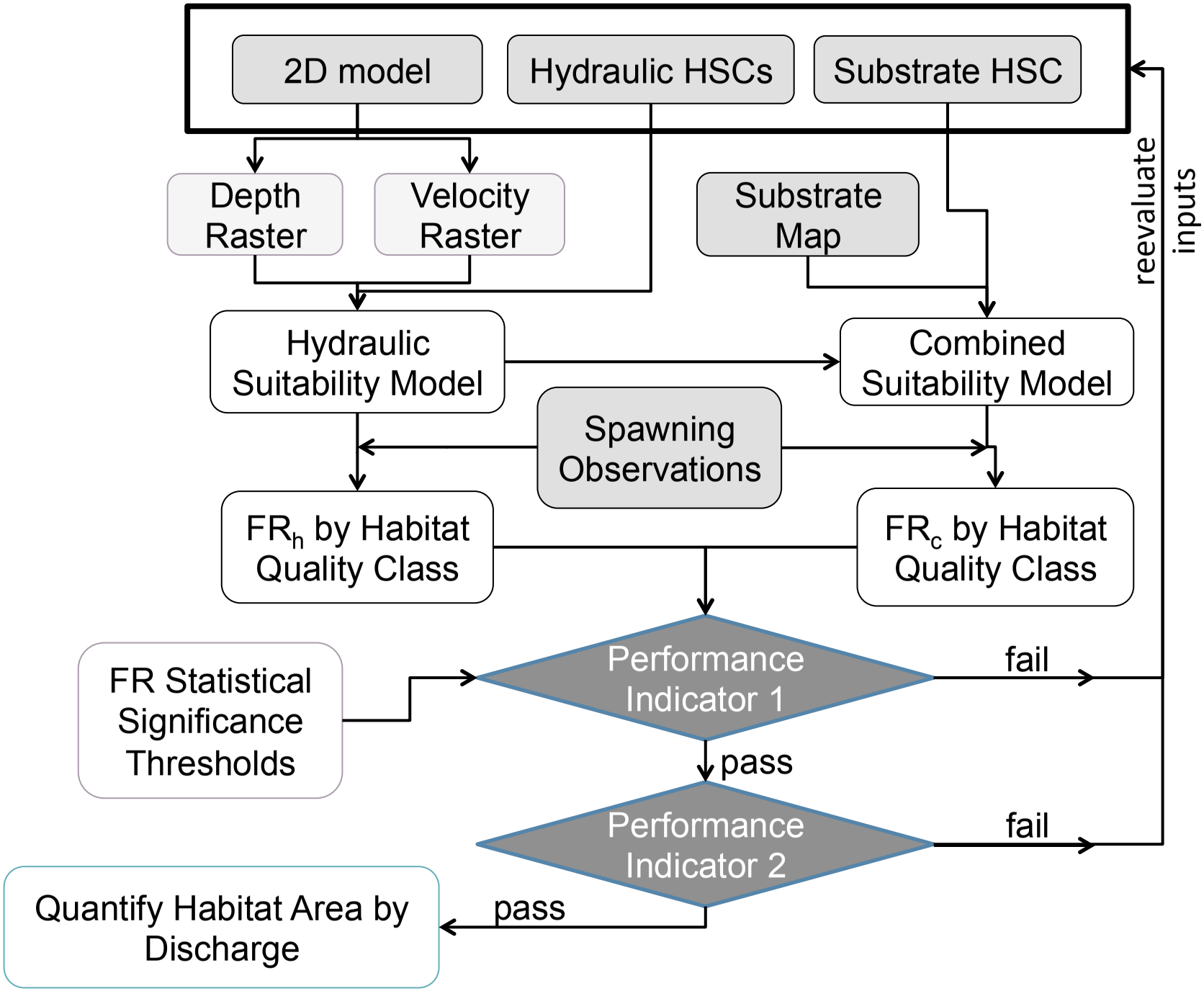
2D model
Hydraulic HSCs
Substrate HSC
Depth Raster
Velocity Raster
Substrate Map
reevaluate inputs
Hydraulic Suitability Model
Combined Suitability Model
Spawning Observations
FRh by Habitat Quality Class
FRc by Habitat Quality Class
FR Statistical Significance Thresholds
Performance Indicator 1
fail
pass
Performance Indicator 2
fail
pass
Quantify Habitat Area by Discharge

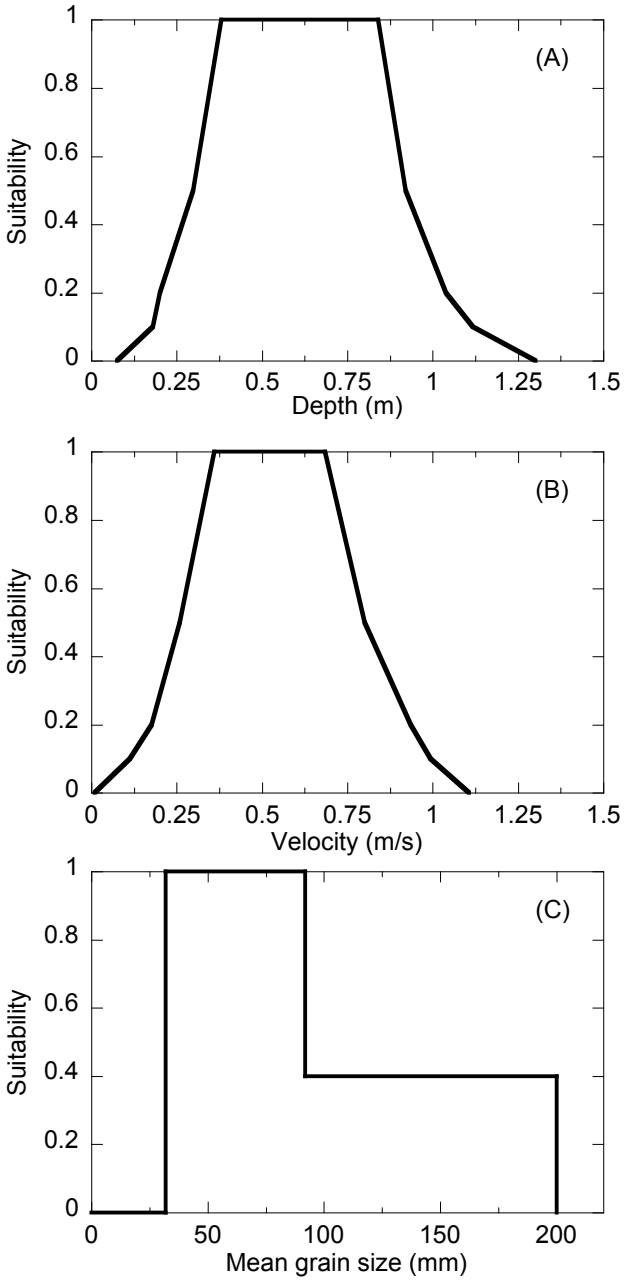
(A)
Suitability
Depth (m)
0
0.2
0.4
0.6
0.8
1
0.25
0.5
0.75
1.25
1.5
(B)
Velocity (m/s)
(C)
50
100
150
200
Mean grain size (mm)

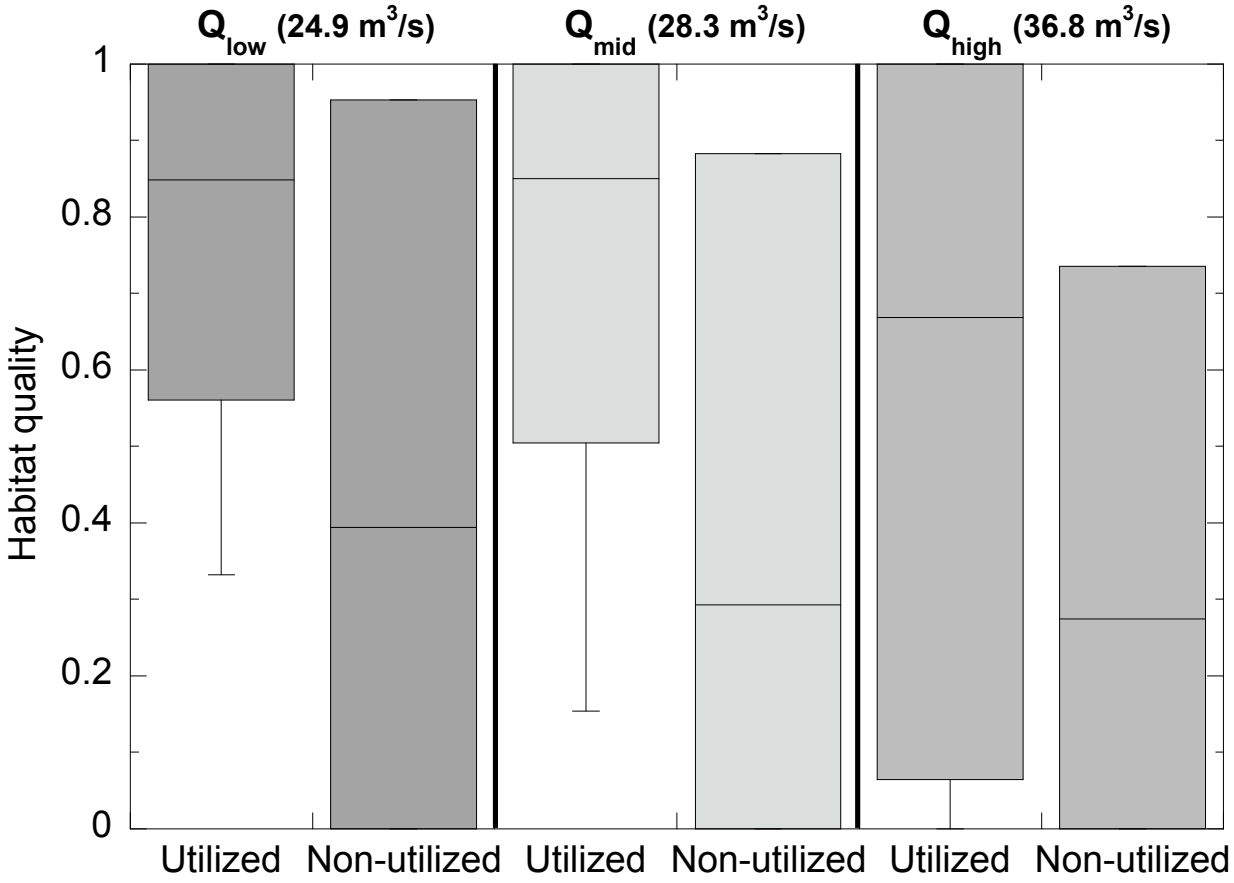
Q_{low} (24.9 m^3/s)
Q_{mid} (28.3 m^3/s)
Q_{high} (36.8 m^3/s)
Habitat quality
1
0.8
0.6
0.4
0.2
0
Utilized
Non-utilized
Utilized
Non-utilized
Utilized
Non-utilized

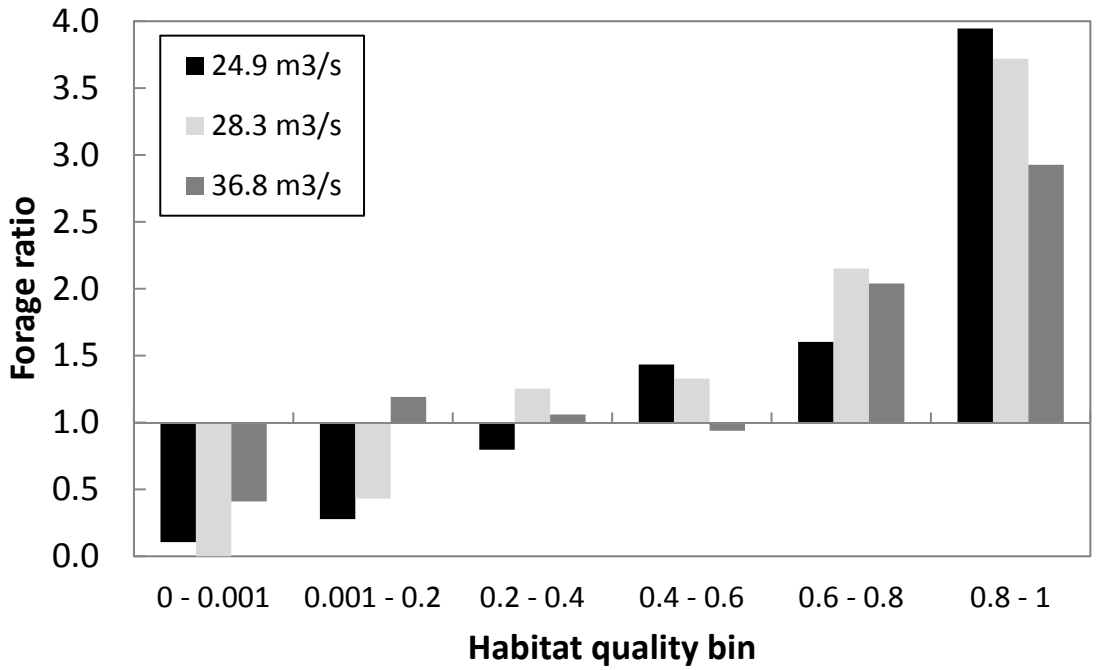
4.0
3.5
3.0
2.5
2.0
1.5
1.0
0.5
0.0
Forage ratio
24.9 m3/s
28.3 m3/s
36.8 m3/s
0 - 0.001
0.001 - 0.2
0.2 - 0.4
0.4 - 0.6
0.6 - 0.8
0.8 - 1
Habitat quality bin

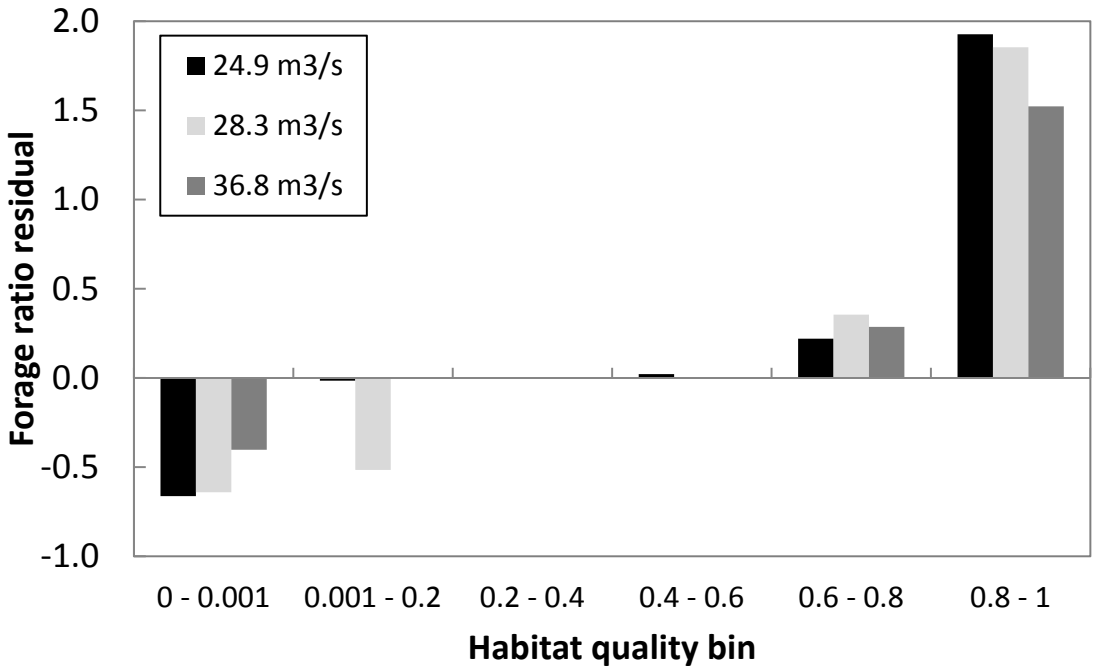
2.0
1.5
1.0
0.5
0.0
-0.5
-1.0
Forage ratio residual
24.9 m3/s
28.3 m3/s
36.8 m3/s
0 - 0.001
0.001 - 0.2
0.2 - 0.4
0.4 - 0.6
0.6 - 0.8
0.8 - 1
Habitat quality bin

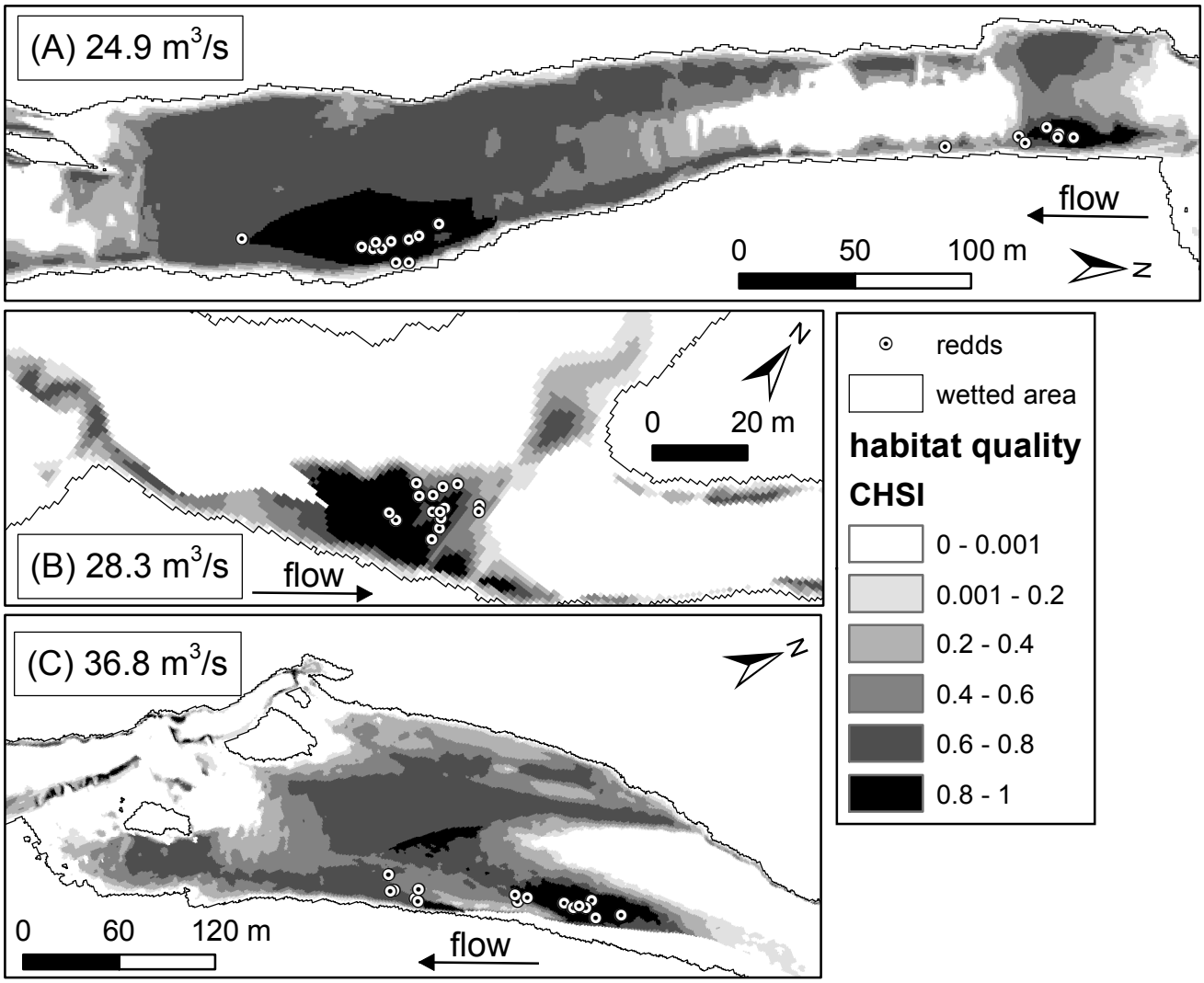
(A) 24.9 m3/s
flow
0
50
100 m
N
(B) 28.3 m3/s
flow
0
20 m
N
(C) 36.8 m3/s
N
0
60
120 m
flow
redds
wetted area
habitat quality
CHSI
0 - 0.001
0.001 - 0.2
0.2 - 0.4
0.4 - 0.6
0.6 - 0.8
0.8 - 1

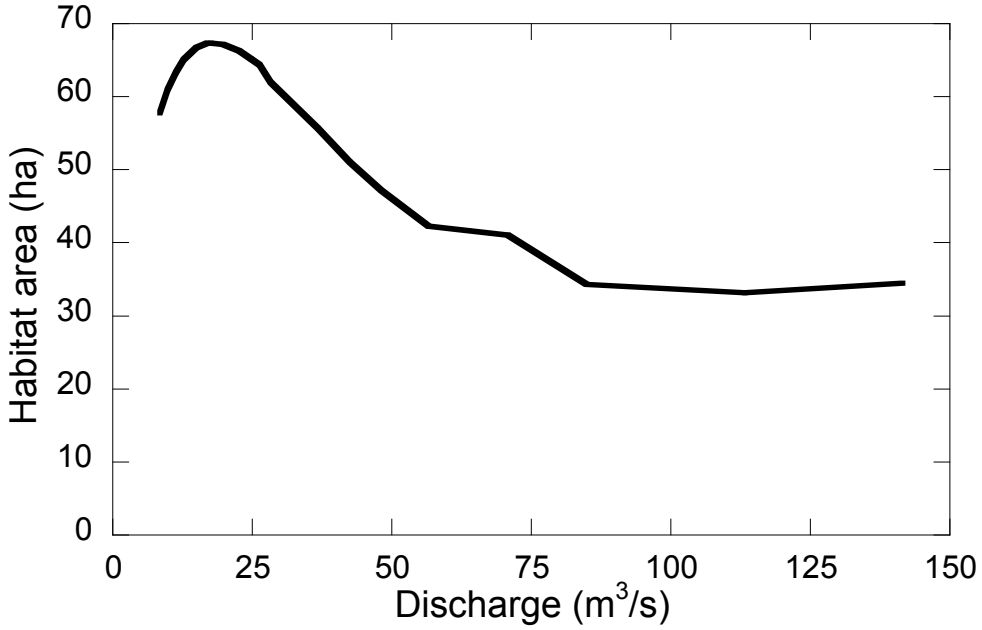
70
60
50
40
30
20
10
0
Habitat area (ha)
0
25
50
75
100
125
150
Discharge (m3/s)

Near-census ecohydraulic bioverification of *Oncorhynchus mykiss* spawning microhabitat preferences.

Supplementary Materials

1 Methods Supplements

1.1 O. mykiss spawning observations

The discharge at which each redd was surveyed was obtained from public flow records, which exist for stations at the head of the LYR (Smartsville gage near Englebright Dam, #11418000) and downstream as close to the terminus but above the zone of backwater effects (Marysville gage, #11421000) through the California Data Exchange Center. The hydrology varied significantly during the study. January through April of 2010 was a relatively dry winter with comparatively low flows throughout the winter; the average discharge over the period was 39.0 m^3/s. There were a few in-channel peak events in January and April. The LYR experienced much higher flows during the 2011 *O. mykiss* spawning season compared to the same period in 2010, with an average discharge (over the time period) of 140.5 m^3/s. There were two notable, sustained overbank floods (~3-4.5 times bankfull discharge) during the 2011 spawning season on March 16 (peak 15-minute discharge=643.0 m^3/s) and April 21 (peak 15-minute discharge=409.4 m^3/s).

1.2 Abiotic data information

Field data collection efforts were explicitly intended to characterize geomorphic, hydrologic, and hydraulic attributes of the LYR at roughly meter-scale resolution in support of a near-census approach to river assessment, including 2D hydrodynamic modeling. The types of data collected included topography and bathymetry (Pasternack 2009; White et al. 2010; Carley et al. 2012) as well as hydraulic data: water surface elevation, depth, velocity magnitude, and velocity direction (Barker 2011; Pasternack et al. 2014). Details about spatial coverage, resolution, and accuracy for the digital elevation model (DEM) used in this study are provided below.

Topographic data came from airborne LiDAR scanning (excluding Timbuctoo Bend) at flows ~ 10–16% of bankfull discharge plus thorough in-water mapping using total stations and RTK GPSs as well as boat-based bathymetry mapping with a single-beam echosounder coupled to an RTK GPS and professional hydrographic software. Basic information describing topographic and bathymetric field data in the Yuba River downstream of Englebright Dam are reported in the box below.

Per traditional standards, water surface elevation observations were obtained from airborne LiDAR and RTK GPS, and depth and depth-average velocity measurements (n= 199) were made at cross-sections. Given the size of the LYR, new methods were developed for more comprehensive model evaluation than traditionally performed, consisting of 5780 measurements of surface velocity direction and magnitude using Lagrangian particle tracking and RTK GPS. This data was carefully vetted for its utility in testing 2D models (Barker 2011).

Attribute	Description
Aerial extent	Entire river, except the Narrows Reach (See Fig. 1 for reach locations)
Years of data collection	Englebright Dam Reach (EDR) was mapped in 2005 and 2007 and Timbuctoo Bend Reach (TBR) was mapped in June–December 2006. From highway 20 down, most bathymetry was mapped in late August to early September 2008, with some high-flow data collection in March and May 2009 as well as small additional near-bank and near-DPD gaps mapped in November 2009. Ground-based topographic surveys were done in November 2008 and November 2009. Lidar of the terrestrial river corridor was flown on September 21, 2008.
Bathymetric Resolution	EDR: Within the 880 cfs inundation area, points were collected along longitudinal lines, cross-sections, and on ~5'x5' grids, yielding an average grid point spacing of one point every 4.5 ft. (54.3 pts/100m^2). TBR: Within the 880 cfs inundation area, points were collected along longitudinal lines, cross-sections, and on ~10'x10' grids, yielding an average grid point spacing of one point every 6.2 ft. (28 pts/100m^2). All else: Within the 880 cfs inundation area, points were collected along longitudinal lines, some cross-sections, and some localized grids. The average grid point spacing is one point every 4.2 ft. (59.8 pts/100m^2).
Topographic Resolution	EDR: Outside the 880 cfs inundation area, points were collected with a combination of grid-based ground-based reflectorless laser scanning of canyon walls and total station surveys of accessible ground, yielding an average grid point spacing of one point every 5.9 ft. (31.3 pts/100m^2). TBR: Outside the 880 cfs inundation area, points were collected on a grid, yielding an average grid point spacing of one point every 9.7 ft. (11.4 pts/100m^2). All else: Outside the 880 cfs inundation area, points were mostly collected with

	lidar, yielding an average grid point spacing of one point every 1.4 ft. (554 pts/100m^2).
Bathymetric Accuracy	EDR: comparison of overlapping echosounder and total station survey points yielded observed differences of 0.2-0.3'. TBR: comparison of overlapping echosounder and total station survey points yielded observed differences of 0.2-0.3'. All else: comparison of overlapping echosounder and total station survey points at one site yielded observed differences of 50% within 0.5', 75% within 0.6', and 94% within 1'. Comparison of boat-based water edge shots versus RTK GPS surveyed water's edge shots yielded observed differences of 75% within 0.1', 91% within 0.2', and 99% within 0.5'.
Topographic Accuracy	EDR: regular total station control point checks yielded accuracies of 0.03-0.06'. TBR: regular total station control point checks yielded accuracies of 0.03-0.06'. All else: compared against 8,769 ground-based RTK GPS observations of elevation along flat surfaces, 54% of LIDAR points were within 0.1' , 86% were within 0.2', and virtually all of the data were within 0.5'. Regular total station control point checks yielded accuracies of 0.03-0.06'. RTK GPS observations had vertical precisions of 0.06'. Comparison of lidar water edge points versus the same for RTK GPS yielded observed differences of 30% within 0.1', 57% within 0.2', and 92% within 0.5'.

1.3 2D hydrodynamic modeling details

The surface-water modeling system (SMS; Aquaveo, LLC, Provo, UT) user interface and sedimentation and river hydraulics–two-dimensional algorithm (Lai 2008) were used to produce these 2D hydrodynamic models of the LYR with internodal mesh spacing of 0.91–1.5 m according to the procedures of Pasternack (2011). SRH-2D is a 2D finite-volume model that solves the Saint Venant equations for depth and velocity at each computational node, and supports a hybrid structured-unstructured mesh that can use quadrilateral and triangular elements of any size, thus allowing for mesh detail comparable to finite-element models. For each model domain a field-observed stage-discharge relation was developed to provide the exit boundary condition. Turbulence closure for the model runs used in this study was achieved using the parabolic, zero equation model, with eddy viscosity varying as a function of depth and shear velocity, modified by an eddy viscosity coefficient (set to 0.6 for the flows simulated in this study) per standard theory and past model performance on the LYR.

For the flows reported in this study, boundary roughness was partially addressed by creating a 0.91-1.53 m resolution DEM, with unresolved roughness addressed by using a constant Manning's roughness value (n) for unvegetated terrain in each reach. Past site-scale 2D models for the LYR using the

54 FESWMS algorithm used an n of 0.043 for the unvegetated, gravel–cobble riverbed (Moir & Pasternack
55 2008; Sawyer et al. 2010). For the long model domains in this study, an evaluation of observed and
56 modeled water surface elevations at a range of in-channel flows up to bankfull found that an n of 0.032
57 best for the bedrock canyon below Englebright Dam, an n of 0.03 best for the valley-confined Timbuctoo
58 Bend, and an n of 0.04 was best downstream of Daguerre Point Dam (Pasternack et al. 2014). Based on
59 LiDAR mapping of the vegetation canopy, the area of vegetation at base flow was ~ 4% and likely
60 consisted of overhanging canopy, so vegetation was not quantified in boundary roughness for flows <
61 28.31 m^3/s. At flows above that indicators of unvegetated boundary roughness showed no difference from
62 that at base flow, so the same unvegetated n values were used. However, airborne LiDAR provided a
63 raster of vegetation canopy height, so a spatially distributed vegetated Manning's roughness value greater
64 than the default unvegetated value was computed using the theory and algorithms explained by Katul et
65 al. (2002) and Casas et al. (2010). This value hinged on the relative depth of inundation of the vegetation
66 canopy in each pixel at each flow, so it was discharge dependent as well. The method and results
67 associated with this modeling technique as applied on the LYR was reported by Abu-Aly et al.
68 (2013).Model simulations were comprehensively validated for flows ranging over an order of magnitude
69 of discharge (0.1 to 1.0 times bankfull) using three approaches: (i) traditional cross-sectional validation
70 methods, (ii) comparison of LiDAR-derived water surface returns against modeled water surface
71 elevations, and (iii) Lagrangian particle tracking with RTK GPS to assess the velocity vectors. Model set-
72 up and performance details are reported in the box below:
73

Attribute	Description
Model domains	For the whole river, there were 5 modeling reaches to make the computational process more efficient. They are given the abbreviations, EDR, TBR, HR, DGR, and FR below. For maps and details about them, see (Pasternack et al. 2014)
Computational Mesh Resolution	EDR: 3' internodal spacing for all Q TBR: For Q<5,000 cfs, 3' internodal spacing. As flow goes overbank, cell size increases to 6'. For flows >21,100 cfs, different mesh has 10' internodal spacing. HR: For flows 0-1300 cfs, 3' internodal spacing. For flows 1300-7500 cfs, 5' internodal spacing. For flows >10,000,

	10' internodal spacing. DGR: For flows 0-1300 cfs, 5' internodal spacing. For flows 1300-7500 cfs, 5' internodal spacing. For flows >10,000, 10' internodal spacing. FR: For flows 0-1300 cfs, 5' internodal spacing. For flows 1300-7500 cfs, 5' internodal spacing. For flows >10,000, 10' internodal spacing.
Discharge Range of Model	EDR was 700 to 110,400 cfs; all else was 300 to 110,400 cfs
Downstream WSE data/model source	EDR: Some WSE observations combined with slope-based translation of the Smartville gage WSE data to the end of the reach. TBR: Direct observation of WSE at a limited number of flows <~12,000 cfs. For higher flows the downstream WSE was taken as the upstream WSE from the HR model at that flow. HR: Continuous direct observation of WSE at flows <~22,000 cfs. For higher flows the downstream WSE was taken as the upstream WSE from the HR model at that flow. DGR: Reach ends exactly at Marysville gaging station, so the WSE data is of the highest quality and abundance. Continuous WSE data for all flows ~500 - 110,400 cfs. FR: Continuous direct observation of WSE at flows <~22,000 cfs. For higher flows the downstream WSE was set to yield an upstream WSE equal to that at the Marysville gage.
River roughness specification	Because the scientific literature reports no consistent variation of Manning's n as a function of stage-dependent relative roughness or the whole wetted area of a river (i.e., roughness/depth), a constant value was used for all unvegetated sediment as follows: 0.032 for EDR (a deeper bedrock canyon), 0.03 for TBR (based on preliminary testing in 2008-2009), and 0.04 for the rest of the LYR (based on validation testing of 0.03, 0.035, 0.04, 0.045, and 0.05 as possible options). For vegetated terrain, the Casas et al. (2010) algorithm was used to obtain a spatially distributed, flow-dependent surface roughness for each model cell on the basis of the ratio of local canopy height to flow depth.
Eddy viscosity specification	Parabolic turbulence closure with an eddy velocity that scales with depth, shear velocity, and a coefficient (e_0) that can be selected between ~0.05 to 0.8 based on expert knowledge and local data indicators. $Q<10{,}000$ cfs: $e_0 = 0.6$ $Q \geq 10{,}000$ cfs: $e_0 = 0.1$
Hydraulic Validation Range	Point observations of WSE were primarily collected at 880 cfs, with some observations during higher flows, but not systematically analyzed. Velocity observations were collected for flows ranging from 530-5,010 cfs. Cross-sectional validation data collected at 800 cfs above DPD and 540 cfs below DPD.
Model mass conservation (Calculated vs	0.001 to 1.98 %

Given Q)	
WSE prediction accuracy	At 880 cfs there are 197 observations. Mean raw deviation is -0.006'. 27% of deviations within 0.1', 49% of deviations within 0.25', 70% within 0.5', 94% within 1'. These results are better than the inherent uncertainty in LiDAR obtained topographic and water surface elevations.
Depth prediction accuracy	From cross-sectional surveys, predicted vs observed depths yielded a correlation (r) of 0.81.
Velocity magnitude prediction accuracy	5780 observations yielding a scatter plot correlation (r) of 0.887. Median error of 16%. Percent error metrics include all velocities (including V <3ft/s, which tends to have high error percents) yielding a rigorous standard of reporting.
Velocity direction prediction accuracy	5780 observations yielding a scatter plot correlation (r) of 0.892. Median error of 4%. Mean error of 6%. 61% of deviations within 5 deg and 86% of deviations within 10 deg.

Using the workflow of Pasternack (2011), SRH-2D model outputs were processed to produce rasters of depth and velocity within the wetted area for each discharge. The first task involved creating the wetted area polygon for each discharge. To do this, depth results were first converted to triangular irregular networks (TIN) and then to a series of 0.9144-m hydraulic raster files. Depth cells greater than zero were used to create a wetted area boundary applied to all subsequent hydraulic rasters. Next, the SRH-2D hydraulic outputs for depth and depth-averaged velocity were converted from point to TIN to raster files within ArcGIS 10.1 staying within the wetted area for each discharge. The complete dataset was a series of 0.9144-m resolution hydraulics rasters derived from SRH-2D hydrodynamic flow simulations at the following discharges: 8.5, 9.9, 11.3, 12.7, 15.0, 17.0, 17.6, 19.8, 22.7, 24.9, 26.3, 28.3, 36.8, 42.5, 48.1, 56.6, 70.8, 85.0, 113.3, 141.6, 212.4, 283.2, 424.8, 597.5, 849.5, 1195.0, 2389.9, and 3126.2 m^3/s.

Despite best efforts with modern technology and scientific methods, the 2D models used in this study have uncertainties and errors. Previously it has been reported that 2D models tend to underrepresent the range of hydraulic heterogeneity that likely exists due to insufficient topographic detail and overly efficient lateral transfer of momentum (Pasternack et al. 2004; MacWilliams et al. 2006). For this study those deficiencies result in a conservative outcome, such that there could be more fine details to the sizes and shapes of peak velocity patches than what is revealed herein. Overall, this study involves model-

based scientific exploration with every effort made to match reality at near-census resolution over tens of km of river length given current technology, but recognizing that current models do have uncertainties.

2 Supplemental References

Abu-Aly, T.R., Pasternack, G.B., Wyrick, J.R., Barker, R., Massa, D., Johnson, T. 2013. Effects of LiDAR-derided, spatially-distributed vegetative roughness on 2D hydraulics in a gravel-cobble river at flows of 0.2 to 20 times bankfull. Geomorphology. doi:10.1016/j.geomorph.2013.10.017.

Barker, J.R. 2011. Rapid, abundant velocity observation to validate million-element 2D hydrodynamic models [M.S. Thesis]. Davis (CA): University of California at Davis.

Carley, J. K., Pasternack, G. B., Wyrick, J. R., Barker, J. R., Bratovich, P. M., Massa, D. A., Reedy, G. D., Johnson, T. R. 2012. Significant decadal channel change 58-67 years post-dam accounting for uncertainty in topographic change detection between contour maps and point cloud models. Geomorphology. doi:10.1016/j.geomorph.2012.08.001.

Casas, A., Lane, S.N., Yu, D., Benito, G. 2010. A method for parameterising roughness and topographic sub-grid scale effects in hydraulic modelling from LiDAR data. Hydrol. Earth Syst. Sci. 14:1567-1579.

Katul, G., Wiberg, P., Albertson, J., Hornberger, G. 2002. A mixing layer theory for flow resistance in shallow streams. Water Resourc. Res. 38:8.

113 Lai, Y.G. 2008. SRH-2D Version 2: Theory and User's Manual. Denver (CO): U.S. Department of the
114 Interior, Bureau of Reclamation, Technical Service Center.

115 MacWilliams, M. L., Wheaton, J. M., Pasternack, G. B., Kitanidis, P. K., Street, R. L. 2006. The
116 Flow Convergence-Routing Hypothesis for Pool-Riffle Maintenance in Alluvial Rivers.
117 Water Resourc. Res. 42. W10427, doi:10.1029/2005WR004391.

118 Moir, H. J. and Pasternack, G. B. 2008. Relationships between mesoscale morphological units,
119 stream hydraulics and Chinook salmon (*Oncorhynchus tshawytscha*) spawning habitat on
120 the Lower Yuba River, California. Geomorphology. 100:527-548.

121 Pasternack, G.B. 2009. Specific Sampling Protocols and Procedures for Topographic Mapping.
122 Marysville (CA): The Lower Yuba River Accord Planning Team.

123 Pasternack, G.B. 2011. 2D Modeling and Ecohydraulic Analysis. Seattke (WA): Createspace.

124 Pasternack, G.B., Wang, C.L., and Merz, J. 2004. Application of a 2D hydrodynamic model to
125 reach-scale spawning gravel replenishment on the lower Mokelumne River, California.
126 River Res. Appl. 20:205-225.

127 Pasternack, G.B., Tu, D., Wyrick, J.R. 2014. Chinook adult spawning physical habitat of the
128 lower Yuba River. Davis (CA): Prepared for the Yuba Accord River Management Team.
129 University of California at Davis.

130 Sawyer, A.M., Pasternack, G.B., Moir, H.J., Fulton, A.A. 2010. Riffle-pool maintenance and
131 flow convergence routing observed on a large gravel-bed river. Geomorphology.
132 114:143-160.

White, J.Q., Pasternack, G.B., and Moir, H.J. 2010. Valley width variation influences riffle-pool location and persistence on a rapidly incising gravel-bed river. Geomorphology. 121:206-221.